

**Best  
Available  
Copy**

J  
A  
S  
O  
N

ADA 016629

Technical Report JSR-74-3

March 1975

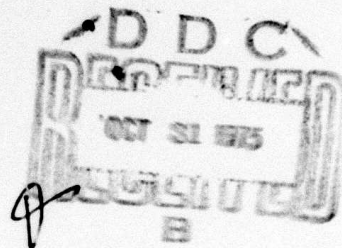
**A COMPUTER CODE TO CALCULATE  
THE EFFECT OF INTERNAL WAVES  
ON ACOUSTIC PROPAGATION**

12

By: STANLEY M. FLATTE FREDERICK D. TAPPERT

Contract No. DAHC15-73-C-0370 ✓  
ARPA Order No. 2504  
Program Code No. 3K10  
Date of Contract: 2 April 1973  
Contract Expiration Date: 30 June 1976  
Amount of Contract: \$2,062,014

Approved for public release; distribution unlimited.



*Sponsored by*

DEFENSE ADVANCED RESEARCH PROJECTS AGENCY  
ARPA ORDER NO. 2504



**STANFORD RESEARCH INSTITUTE**  
Menlo Park, California 94025 • U.S.A.

*Copy No. 200*

The views and conclusions contained in this document are those of the authors and should not be interpreted as necessarily representing the official policies, either expressed or implied, of the Defense Advanced Research Projects Agency or the U.S. Government.



REPORT DOCUMENTATION PAGE		READ INSTRUCTIONS BEFORE COMPLETING FORM
1. REPORT NUMBER JRS-74-3	2. GOVT ACCESSION NO.	3. RECIPIENT'S CATALOG NUMBER
4. TITLE (and subtitle) A COMPUTER CODE TO CALCULATE THE EFFECT OF INTERNAL WAVES ON ACOUSTIC PROPAGATION		5. TYPE OF REPORT & PERIOD COVERED Technical Report
6. AUTHOR(S) Stanley M. Flatté Frederick D. Tappert		7. PERFORMING ORG. REPORT NUMBER SRI - 3000
8. PERFORMING ORGANIZATION NAME AND ADDRESS Stanford Research Institute Menlo Park, California 94025		9. CONTRACT OR GRANT NUMBER(s) DAHC15-73-C-0370 HIPC 73-2544
10. CONTROLLING OFFICE NAME AND ADDRESS Defense Advanced Research Projects Agency 1400 Wilson Boulevard Arlington, Virginia 22209		11. PROGRAM ELEMENT, PROJECT, TASK AREA & WORK UNIT NUMBERS 11/111 75 12/62p.
12. REPORT DATE June 1975		13. NO. OF PAGES 80
14. MONITORING AGENCY NAME & ADDRESS (if diff. from Controlling Office)		15. SECURITY CLASS. (of this report) UNCLASSIFIED
16. DISTRIBUTION STATEMENT (of this report) Approved for public release; distribution unlimited.		17. DISTRIBUTION STATEMENT (of the abstract entered in Block 20, if different from report)
18. SUPPLEMENTARY NOTES		
19. KEY WORDS (Continue on reverse side if necessary and identify by block number) Ocean acoustics Acoustic propagation Acoustic fluctuations Internal waves      Computer simulation Vertical arrays		
20. ABSTRACT (Continue on reverse side if necessary and identify by block number) The signal received by a hydrophone in the ocean many kilometers from a steady sound source fluctuates dramatically due to variations of the speed of sound in sea-water. We have written a computer code that simulates the passage of acoustic CW signals through an ocean with internal waves. The code generates a sound-speed field from an internal-wave spectrum that has been derived from oceanographic measurements. The acoustic propagation is achieved through the use of the parabolic-equation approximation. The code is limited fundamentally to acoustic		

DD FORM 1 JAN 73 1473

EDITION OF 1 NOV 65 IS OBSOLETE

333500

20 ABSTRACT (Continued)

10 Hz, and by practical computer-time constraints to frequencies below  $\sqrt{400}$  Hz. The code allows the calculation of the amplitude and phase of the full acoustic field as a function of depth and range at any desired time.

## CONTENTS

DD FORM 173

LIST OF ILLUSTRATIONS . . . . .	v
LIST OF TABLES . . . . .	vi
I      INTRODUCTION . . . . .	1
II     OCEAN SOUND-SPEED STRUCTURE . . . . .	3
A.    Deterministic Profile . . . . .	3
B.    Internal Waves. . . . .	4
C.    Final Expression for Sound-Speed Structure. . . . .	7
III    THE PARABOLIC-EQUATION METHOD. . . . .	8
A.    Introduction. . . . .	8
B.    Approximations and Ranges of Validity . . . . .	8
C.    Analogy with Quantum Mechanics. . . . .	11
IV    NUMERICAL REALIZATION OF THE INTERNAL-WAVE MODEL . . . . .	13
A.    Eigenfunction Determination . . . . .	13
B.    Range of $j$ and $k$ . . . . .	13
C.    Generation of $\delta c_{IW}$ . . . . .	13
V    NUMERICAL PROPAGATION OF THE ACOUSTIC FIELD USING THE PARABOLIC EQUATION . . . . .	16
A.    Algorithm . . . . .	16
B.    Acoustic Source . . . . .	17
C.    Surface Boundary Condition. . . . .	17
D.    Bottom Absorption . . . . .	17
E.    Number of Depth Points. . . . .	18
F.    Size of Range Step. . . . .	18

VI	FORMAT OF SAVED DATA FROM COMPUTER RUNS . . . . .	19
VII	COMPUTER RUNNING TIMES. . . . .	22
VIII	CODE ORGANIZATION AND LISTING . . . . .	23
Appendix	CUBIC SPLINE INTERPOLATION . . . . .	41
References	. . . . .	46
Figures	. . . . .	57
Distribution List	. . . . .	67

LIST OF ILLUSTRATIONS

Figure 1 Deterministic Sound-Speed Profile as a Function of Ocean Depth. . . . .	57
Figure 2 Sound-Speed Profiles Due to Internal-Wave Modes. . . . .	58
Figure 3 Internal-Wave Spectrum as a Function of Mode Number $j$ and Horizontal Wave-Number $k$ . . . . .	59
Figure 4 Typical Sound-Speed Fluctuation Profile Induced by Internal Waves . . . . .	60
Figure 5 Analogy Between (a) An Acoustic Ray Propagating in a Sound Channel Characterized by $c(z)$ , and (b) A Schrödinger-Equation Wave Packet in a Potential Well $V(z)$ . . . . .	61
Figure 6 Analogy Between (a) An Acoustic-Wave Function Traveling Down the Sound Channel Without Spreading in Depth, and (b) A Schrödinger-Equation Ground-State Wave Function in a Potential Well $V(z)$ . . . . .	62
Figure 7 Diagram of Boundary Conditions and Source Geometry in Our Numerical Simulation. . . . .	63
Figure 8 Code Organization. . . . .	64

LIST OF TABLES

Table 1	Identification Record. . . . .	20
Table 2	Data Record. . . . .	21

## I INTRODUCTION

Sonar has been used for detection and communication in the ocean for many years. The effect on sonar of a geographical variation in the sound-speed profile of the ocean has received considerable attention as more precise and sensitive use has been made of acoustic signals in the ocean. However, relatively little attention has been focused on the smaller-scale variations in the oceans--in particular, the internal waves, which not only provide variations in space (on scales of a few hundred meters vertically and a few kilometers horizontally), but also introduce the new dimension of time variability (on a scale of a few hours).

The theory of sound propagation through internal waves has not yet been fully developed, so that many questions of a qualitative nature are open. We have written a computer code to answer some of these questions, taking advantage of the advent of the use of the parabolic equation method in underwater acoustics,<sup>1-3\*</sup> and the existence of internal-wave models derived from oceanographic measurements.<sup>4</sup> With certain restrictions (to be described) the full acoustic-wave field can be propagated through an ocean with variable sound speed, and the resulting long-range transmission characteristics can be studied.

---

\* References are listed at the end of the report.

Consider the acoustic pressure in the ocean as  $p(r, t)$ . The wave equation for  $p$  is

$$\nabla^2 p - \frac{1}{c^2} \frac{\partial^2 p}{\partial t^2} = 0 ,$$

where it has been assumed that the sound speed  $c(r, t)$  varies slowly with position and that the water density, as far as its effect on inertia is concerned, is essentially constant. Hence, the quantity that determines the structure and behavior of the pressure is the sound speed  $c(r, t)$ .

In the following sections we present a model for the expected sound-speed structure in the ocean, the parabolic equation approximation to the wave equation and the reasons it is valid for our model of the sound-speed structure, and the computer code that has combined the model of internal waves and the parabolic equation method into a useful apparatus for studying oceanic sound transmission.

Initial results obtained through use of our code are given in Reference 6.

## II OCEAN SOUND-SPEED STRUCTURE

### A. Deterministic Profile

On the scale of the depth of the ocean (4 to 5 km) the sound speed as a function of depth,  $z$ , is determined by the gross behavior of the density, temperature, and salinity. We use the profile derived by Munk,<sup>5</sup> whose input is an exponentially decreasing density gradient. The resulting "canonical" profile is

$$c_{CP}(z) = c_1 \left\{ 1 + \epsilon [e^{-\eta} - (1-\eta)] \right\}$$

$$\text{where } \eta = \frac{z-z_A}{\frac{1}{2}B}.$$

Note that  $c(z)$  has a minimum at  $z_A$ , that the width of the minimum is  $B$ , and that the deviation of the sound speed from the minimum value  $c_1$  is of order  $\epsilon$ .

Typical (though not universal) values for the parameters are:

$$z_A = 1300 \text{ m}$$

$$B = 1300 \text{ m}$$

$$\epsilon = 0.74 \times 10^{-2}$$

$$c_1 = 1500 \text{ m/s}$$

See Figure 1\* for a graph of  $c_{CP}(z)$  using these parameters.

---

\* Illustrations are grouped at the end of the report.

One must point out that realistic ocean profiles in most cases have significantly different behavior from this general form. For example, within a few hundred meters of the surface a mixed layer usually results in a lowered sound-speed gradient. However, we ignore these details in the present version of the code.

### B. Internal Waves

The density gradient in the ocean leads to the possibility of waves traversing the volume of the ocean just as the density discontinuity at the surface leads to the possibility of surface waves. The density gradient is usually presented in the form

$$N(z) \equiv \left\{ -\frac{g}{\rho_0} \frac{\partial \rho}{\partial z} \right\}^{1/2}$$

where  $N(z)$  is called the local stability (Brunt-Väisälä) frequency.

Munk's model for  $N(z)$  is

$$N(z) = n_0 e^{-z/B}$$

where  $n_0 = 4$  cycles/hr.

Let  $\vec{w}(r, t)$  be the displacement of a particular density level from its mean position. It can be shown that  $w$  satisfies the equation:

$$\frac{\partial^2}{\partial t^2} \left( \nabla^2 w \right) + N^2(z) \nabla_h^2 w = 0$$

The eigenmodes of this equation can be found by taking

$$w = W(j, k, z) e^{i[k_1 x + k_2 y - \omega(j, k) t]}$$

where  $k = \sqrt{k_1^2 + k_2^2}$  = horizontal wave number.

Substituting, we have

$$W'' + \frac{\frac{N^2(z) - \omega^2}{2}}{\omega} k^2 W = 0$$

Modifying this equation to account for the rotation of the earth we find

$$W'' + \left( \frac{\frac{N^2(z) - \omega^2}{2}}{\omega^2 - \omega_i^2} \right) k^2 W = 0$$

where  $\omega_i$  = inertial frequency = (2 cycles/day)sin(latitude).

Boundary conditions are  $W(z) = 0$  at surface and bottom. Thus, for a given horizontal wave number there are a discrete infinity of solutions to this equation labeled by the mode number  $j$ , with frequencies  $\omega(j, k)$ . The sound-speed fluctuation profiles caused by each internal wave will follow the depth structure of  $N^2(z)W(j, k, z)$ . Several examples of such profiles are shown in Figure 2.

The sound velocity fluctuations caused by a full internal-wave field will be

$$\delta c_{IW} = \operatorname{Re} \left\{ \sum_{j, k_1, k_2} B(j, k_1, k_2) e^{i[k_1 x + k_2 y - \omega(j, k)t]} N^2(z) W(j, k, z) \right\}.$$

The difficulty of integrating this distribution over the  $x-z$  plane (because we will propagate sound only in the  $x-z$  plane with the acoustic transmission code) has caused us to consider a simplified version of the internal-wave spectrum where internal waves are propagated only in (or opposite to) the direction that the sound waves propagate. In addition,

we combine real and imaginary parts to reduce fluctuations in the overall energy in the internal waves as a function of time:

$$\delta c_{1W} = \frac{c_1}{\sqrt{2}} \left\{ \operatorname{Re} \Delta + \operatorname{Im} \Delta \right\}$$

$$\Delta = \sum_{j,k} A(j,k) W(j,k,z) N^2(z) e^{i[kr - \omega(j,k)t]}$$

where  $W(j,k,z)$  is normalized so that  $\int_0^{z_{\max}} N^4(z) W^2(j,k,z) dz = 1$ .

The  $A(j,k)$  are complex Gaussian random variables. From a synopsis of diverse oceanographic measurements, Garrett and Munk<sup>4</sup> have proposed the following model:

$$\langle A(j,k) A^*(j',k') \rangle = \delta_{jj'} \delta_{kk'} \frac{2\pi}{3L} \left[ \left\langle \left( \frac{\delta c}{c} \right)^2 \right\rangle \Big|_{z=0} \right]$$

$$\frac{4\omega_i^2 j^{\alpha-1} (j_*)^{\alpha-1}}{n_o (j+j_*)^\alpha \left[ k^2 + \left( \frac{\pi\omega_i j}{n_o B} \right)^2 \right]^2}$$

$$\left\langle \left( \frac{\delta c}{c} \right)^2 \right\rangle \Big|_{z=0} = (4 \times 10^{-4})^2$$

where  $j_* = 3$ ,  $\alpha = 2.5$ , and  $L$  is the horizontal periodicity length over which the internal waves are generated (because we are generating  $k$  in discrete steps rather than as a continuum). The relative intensity of the various modes is shown in Figure 3.

Note that the magnitude of the sound-speed fluctuation due to internal waves is  $\delta c/c \sim 10^{-4}$ , a factor of one hundred below the magnitude of the deterministic structure. Also the spatial behavior of the sound-speed variations due to internal waves is of the order of a few hundred meters vertically and several kilometers horizontally. Internal-wave frequencies vary from  $n_0 = 4$  cycles/hr for the lowest mode to one cycle/day for the high modes ( $j \sim 20$ ). Figure 4 shows some typical sound-speed profiles due to internal waves.

### C. Final Expression for Sound-Speed Structure

The sound speed as a function of position and time is given by

$$c(\vec{r}, t) = c_{CP}(z) + \delta c_{IW}$$

$$= c_1 \left( 1 + \frac{\delta c}{c} \right)$$

where

$$\frac{\delta c}{c} \equiv \underbrace{\varepsilon \left[ e^{-\gamma} - (1-\gamma) \right]}_{O(10^{-2})} + \underbrace{\frac{\delta c_{IW}}{c_1}}_{O(10^{-4})}$$

Hence, the deviation in sound speed from a constant value is always small, and we may write, for example,

$$\frac{1}{c^2} = \frac{1}{(c_1)^2} \left\{ 1 - \frac{2\delta c}{c} \right\} .$$

This expression will of course appear in the wave equation.

## III THE PARABOLIC-EQUATION METHOD

A. Introduction

The parabolic-equation method was originally developed by Leontovich and Fok in 1946 to study long-range propagation of radio waves in the troposphere.<sup>1</sup> This method was introduced into the field of underwater acoustics by Tappert in 1972, and a computer program based on this method was developed by Tappert and Hardin to solve acoustic propagation problems of interest to the Navy.<sup>2,3</sup>

B. Approximations and Ranges of Validity

The wave equation for acoustic pressure  $\vec{p}(\vec{r}, t)$  is

$$\nabla^2 p - \frac{1}{c^2} \frac{\partial^2 p}{\partial t^2} = 0 .$$

Since the time variation of  $c$  takes place over hours, and the acoustic frequencies will be in the range of  $\sim 200$  Hz, we may treat sound propagation at any time as though the ocean structure were frozen.

Hence, a particular acoustic frequency  $\omega$  would be unaffected by the ocean and we may set

$$p = p' e^{-i\omega t}$$

$$\Rightarrow \nabla^2 p' + k^2 p' = 0 \quad \text{where } k \equiv \frac{\omega}{c} .$$

$$\text{but } k^2 = \frac{\omega^2}{c_1^2} \left(1 - \frac{2\delta c}{c}\right) = k_o^2 \left(1 - \frac{2\delta c}{c}\right)$$

$$\Rightarrow \nabla^2 p' + k_o^2 p' - 2k_o^2 \frac{\delta c}{c} p' = 0 .$$

Neglecting the  $\delta c/c$  term initially, the solution in cylindrical coordinates is

$$p' \propto H_o(k_o r) \sim \frac{e^{ik_o r}}{\sqrt{r}}$$

so we try for the full solution:

$$p' = \psi_t(r, z, \varphi) H_o(k_o r)$$

where the reduced wave function  $\psi$  is labeled by the time  $t$ , because the  $\delta c/c$  structure of the ocean is different for different times. Substituting  $p'$  in the full equation we find:

$$H_o \nabla^2 \psi + \psi \nabla^2 H_o + 2 \frac{\partial H_o}{\partial r} \frac{\partial \psi}{\partial r} + k_o^2 H_o \psi - 2k_o^2 \frac{\delta c}{c} H_o \psi = 0$$

If  $k_o r \gg 1$ ,

$$\frac{\partial H_o}{\partial r} = ik_o \left(1 - \frac{1}{2ik_o r} + O\left(\frac{1}{k_o^2 r^2}\right)\right) H_o$$

$$\Rightarrow \nabla^2 \psi - \frac{1}{r} \frac{\partial \psi}{\partial r} + 2ik_o \frac{\partial \psi}{\partial r} - 2k_o^2 \frac{\delta c}{c} \psi = 0$$

$$\frac{\partial^2 \psi}{\partial r^2} + \frac{1}{r^2} \frac{\partial^2 \psi}{\partial \varphi^2} + \frac{\partial^2 \psi}{\partial z^2} + 2ik_o \frac{\partial \psi}{\partial r} - 2k_o^2 \frac{\delta c}{c} \psi = 0 .$$

The key to the parabolic-equation method involves the following physical approximations, based on the structure of  $\delta c/c$ :

- $k_o r \gg 1$

- $\frac{\partial^2 \psi}{\partial r^2} \ll 2ik_o \frac{\partial \psi}{\partial r}$

Valid if the objects off which the acoustic waves are scattering have sizes that are much larger than a wavelength. This is equivalent to having only relatively forward scattering, which results in small changes in  $\psi$  over an acoustic wavelength. Let  $L_v$  be the vertical scale of sound speed variations. Then  $k_o L_v \gg 1$  is required. Note that energy scattered at large angles is removed by the ocean bottom anyway.

- $\frac{\partial^2 \psi}{\partial r^2} \approx \frac{1}{r^2} \frac{\partial^2 \psi}{\partial \phi^2} \ll \frac{\partial^2 \psi}{\partial z^2}$

This is true because the canonical profile, which is 100 times larger than the sound-speed fluctuation of the internal waves, affects the  $z$  coordinate only. More importantly, however, the internal-wave gradients in the vertical are an order of magnitude greater than the horizontal.

The approximate wave equation is therefore

$$-\frac{1}{2k_o} \frac{\partial^2 \psi}{\partial z^2} + k_o \frac{\delta c}{c} \psi = i \frac{\partial \psi}{\partial r} . \quad (1)$$

To summarize the approximations required for this parabolic equation to be valid, we need the following quantities:

$\omega_{IW}$  = Largest frequency involved in the internal-wave spectrum  
 $\approx 4$  cycles/hr

$L_H$  = Minimum horizontal scale of sound-speed fluctuations  
 $\approx 1$  km

$L_V$  = Minimum vertical scale of sound-speed fluctuations  
 $\approx 200$  m.

Validity of the parabolic equation requires:

$$(1) \omega \gg \omega_{IW}$$

$$(2) k_o r \gg 1$$

$$(3) L_H \gg L_V$$

$$(4) k_o L_V \gg 1$$

Requirement 3 is well satisfied by our internal-wave model. Requirement 4 sets a lower limit on the frequency we can treat:

$$freq \gg \frac{1}{2\pi} \frac{c}{L_V} \approx 1 \text{ Hz}$$

Requirement 1 is subservient to Requirement 4. Requirement 2 sets a lower limit on the range of sound transmission:

$$R \gg \frac{1}{k_o} \approx 25 \text{ m for 10 Hz}$$

Thus, any experiments with frequencies of 10 Hz or higher over ranges of  $(10)/k_o$  or longer should be well treated by the parabolic equation. This includes all problems of interest at present.

### C. Analogy with Quantum Mechanics

The Schrödinger equation in nonrelativistic quantum mechanics is

$$-\frac{1}{2m} \frac{\partial^2 \psi}{\partial z^2} + V(z)\psi = i \frac{\partial \psi}{\partial t} . \quad (2)$$

We see that our parabolic equation (1) is of the same form if the analogies are made as follows:

$$\text{Mass} = k_o$$

$$\text{Potential} = k_o \frac{\delta c}{c}$$

Time = range

Energy level = horizontal wave number

$$\text{Momentum} = \text{angle} \left( \frac{dz}{dr} \right) .$$

Many characteristics of underwater acoustics can be easily understood on the basis of this analogy. We will give two examples for transmission with  $\delta c/c$  given by the canonical profile (no internal waves):

- (1) Rays--Consider a narrow wave packet with velocity  $v$  propagating in our potential well [see Figure 5(b)]. As long as  $\frac{1}{2}mv^2 < V_{\max}$  the packet will bounce back and forth inside the well. The analogy says that as long as  $\frac{1}{2}k_o\theta \ll k_o (\delta c/c)_{\max}$ , a ray starting from the sound axis with  $\theta$  will be contained within the sound channel [see Figure 5(a)].
- (2) Ground State--Forming a wave packet with the form  $\psi_o(z)$  where  $\psi_o$  is the ground-state wave function of the potential  $V(z)$  would result in an acoustic field propagating in range with no change in structure--i.e., no spreading of the wave packet (see Figure 6).

## IV NUMERICAL REALIZATION OF THE INTERNAL-WAVE MODEL

A. Eigenfunction Determination

A program (ZMODE)<sup>7</sup> was used to numerically generate the eigenfunctions  $w(j, k, z)$  and frequencies  $\omega(j, k)$ . Several modifications to ZMODE were required:

- (1) An increase of dimensions so that 128 values of  $k$  and 256 values of  $z$  can be treated.
- (2) Inclusion of the inertial frequency  $\omega_i$ .
- (3) Change of the initial guess for  $\omega(j, k)$ .  $|y_m(0) = (m-\frac{1}{4})\pi$  instead of  $(m-\frac{1}{2})\pi$ .|

B. Range of  $j$  and  $k$ 

Modes with  $1 \leq j \leq 24$  are included. Values of  $k$  range from  $(k_{\max}/128)$  to  $(127/128)k_{\max}$  in 127 equal steps. Both positive and negative values of  $k$  are included, making a total of 254 values of  $k$ . The value of  $k_{\max}$  is 1 cycle/km at present. Thus a total of  $254 \times 24$ , or 6096 separate modes, are generated.

C. Generation of  $\delta c_{IW}$ 

The steps in generating the sound-speed deviations caused by internal waves,  $\delta c_{IW}$ , are as follows:

- (1) The 6096 different  $A(j, k)$  are generated according to a Rayleigh probability distribution in amplitude, and

variance given by the spectrum described in Section II. The phase angle of each  $A(j,k)$  is randomly generated in the region 0 to  $2\pi$ . Thus, 12192 random numbers are needed.

(2) For each  $j$  value, the values of  $k$  are stepped through, calculation of the function  $W(j,k,z)$  is accomplished, and a matrix element is incremented until the following complex matrix is completed:

$$M(k,z) = \sum_j A(j,k) N^2(z) W(j,k,z) e^{i\omega(j,k)t}$$

(3) The value of  $\delta c_{IW}$  at range  $r$  and depth  $z$  is the Fourier transform of  $M(k,z)$ :  $\Delta(r,z) = \sum M(k,z) e^{ikr}$ . The matrix  $\Delta$  is calculated from  $M$  by the fast-Fourier-transform technique. The values of  $r$  at which  $\Delta$  is known are  $0 < r < 256\pi/k_{\max}$  in steps of  $\pi/k_{\max}$ . In the present code this means  $0 < r < 128$  km; the code simply repeats the structure it has, every 128 km.

We repeat that

$$\delta c_{IW} = \frac{c_1}{2} [\text{Re}\Delta + \text{Im}\Delta]$$

Hence we have the internal-wave sound-speed deviations at time  $t$  on a grid of 128 km by 4 km with 256 points horizontally and 256 points vertically. (Step size  $\sim 16$  m vertically and 0.5 km horizontally.)

(4) The propagation section of the code may need the value of  $\delta c_{IW}$  on points off the above grid. The code allows division of the grid into a finer grid by powers of two, with the values of  $\delta c_{IW}$  on the fine grid being obtained by cubic spline interpolation (see Appendix).

(5) The  $256 \times 256$  grid of  $\delta c_{IW}$  values is kept in Large Core memory for fast access during the sound-propagation phase of the code. When the values of  $\delta c_{IW}$  at a new time  $t$  are desired, the entire procedure is repeated with a new time  $t$ , with two exceptions; first, the random numbers do not need to be generated again, and second, the eigenvalues  $\omega(j,k)$  do not need to be calculated again because they have been saved in computer memory. Due to storage limitations, however, the functions  $W(j,k,z)$  must be recalculated at every  $t$ , since they have not been saved.

V NUMERICAL PROPAGATION OF THE ACOUSTIC FIELD  
USING THE PARABOLIC EQUATION

A. Algorithm

We must numerically solve the parabolic equation

$$\frac{\partial \Psi}{\partial r} = \frac{1}{2k_0} \frac{\partial^2}{\partial z^2} - ik_0 \frac{\delta c}{c} \Psi = i(A + B)\Psi$$

where reference to the variable  $z$  is suppressed, and where  $A$  and  $B$  are real operators. The first-order solution, useful for a numerical method, is:

$$\Psi(r+dr) = e^{iA \frac{dr}{2}} e^{iBdr} e^{iA \frac{dr}{2}} \Psi(r)$$

Since step follows step, we use

$$\Psi(r+dr) = e^{iA dr} e^{iB dr} \Psi(r)$$

Evaluation of  $e^{iB dr}$  is straightforward--it is a complex number with unit modulus. Evaluation of  $e^{iA dr}$  is more complicated since  $A$  is a differential operator:

$$e^{iA dr} \phi(z) = F^{-1} e^{i\hat{A} dr} F[\phi(z)]$$

$F$  is a fast-Fourier-transform operation, and

$$\hat{A} = -\frac{i}{2k_0} k^2$$

in  $k$ -space.

This algorithm is fast, and also it is very stable, since the total acoustic energy

$$\int |\psi|^2 dz$$

is exactly conserved as a function of  $r$ . This is because the operations on  $\psi(r)$  are exactly unitary.

#### B. Acoustic Source

The acoustic field may be started with any function of depth. The present code models a point source, at a depth provided as input, with unit strength at 1 yard.

#### C. Surface Boundary Condition

The reduced wave function  $\psi$  must be exactly zero at the ocean surface (pressure release boundary condition). In order to ensure the proper application of this condition, a "reflected ocean" is carried along with the real ocean. In the reflected ocean is an image source of the same strength as the real source, but reflected in position and  $180^\circ$  out of phase with the real source (see Figure 7).

#### D. Bottom Absorption

In order to avoid reflection off the ocean bottom, a gradual loss of intensity is imposed on  $\psi(z)$  as  $z$  nears the ocean bottom. The functional form of the imposed loss is

$$\psi(r+dr) = L(z) e^{iA dr} e^{iB dr} \psi(r)$$

$$L(z) = \exp \left\{ -\alpha dr e^{-\left(\frac{z-z_{\max}}{s}\right)^2} \right\} .$$

The code has at present

$$\alpha = 0.05/m$$

$$\theta = 0.04 z_{\max}$$

This form effectively stops any acoustic energy from penetrating below about 500 m above the bottom. Even this form does cause some reflection off the bottom at a low-intensity level, for long-wavelength sound.

E. Number of Depth Points

The maximum number of depth points in the real ocean allowed by the code is 1024 (the number used must be a power of two).

F. Size of Range Step

The size of the range step should not be too large or the numerical algorithm will break down. Experience has indicated that 0.5 km is a safe step at 100 Hz and 0.25 km is safe at 400 Hz.

## VI FORMAT OF SAVED DATA FROM COMPUTER RUNS

As the sound-propagation code is run, various quantities are put on magnetic tape, much in the manner of an actual field experiment. The tapes can then be separately analyzed.

At the present the output consists of the following logical records:

- (1) An identification record (see Table 1).
- (2) A number of data records containing the acoustic field at various points (see Table 2). For each time step the full acoustic field is output for 12 values of the range, and the acoustic field at four selected depths is output for all values of the range.
- (3) An end-of-file mark.

Table 1  
IDENTIFICATION RECORD

Word Number	Quantity	Format
1	Number of words following	I
2	Frequency (Hz)	F
3	$c_1$ (m/s)	F
4	$z_{\max}$ (m)	F
5	GW (m)	F
6	FGW (m)	F
7	dr (m)	F
8	$k_o$ (m <sup>-1</sup> )	F
9	dz (m)	F
10	$\lambda$ (m)	F
11	$\tau$	F
12	Source depth (m)	F
13	Number of depth points	I
14	$\log_2 N$	I
15	-	
16	-	
17	-	
18	$c_1$ (m/s)	F
19	$z_A$ (m)	F
20	B (m)	F
21	$g$ (s <sup>-1</sup> )	F
22	$N_o$ (s <sup>-1</sup> )	F
23	$\omega_i$ (s <sup>-1</sup> )	F
24	-	F
25	$z_{\max}$	F

Table 1 (Concluded)

Word Number	Quantity	Format
26	NZ (internal waves)	I
27	$k_{\max}$	F
28	NK (internal waves)	I
29	NMODE (internal waves)	I
30	$[\langle (\delta c/c)^2 \rangle  _{z=0}]^{\frac{1}{2}}$	F
31	TIW	F
32	$j_*$	I
33	Number of range steps	I
34	Number of time steps	I
35	-	
36	Time-step interval	F

Table 2

## DATA RECORD

Word	Quantity
1	Number of following words
2	$r$ (m)
3	$t$ (s)
4 - 1027	$\text{Re}\{\psi(z_i)\}$ starting from ocean surface
1028 - 2051	$\text{Im}\{\psi(z_i)\}$ starting from ocean surface
2052 - end	$\text{Re}\psi(z_a, r_1), \text{Im}\psi(z_a, r_1), \text{Re}\psi(z_a, r_2), \text{Im}\psi(z_a, r_2) \dots$ until all ranges since the last tape output are included for selected depth $z_a$ . Then the same list for selected depths $z_b$ , $z_c$ , and $z_d$ . (Maximum number of range steps between tape outputs is set at 100.)

## VII COMPUTER RUNNING TIMES

The breakdown of the CDC 7600 computer time to run the code is as follows:

- (1) To generate the  $\delta C_{IW}$  on a  $256 \times 256$  grid for each time:  
28 CPU seconds.
- (2) To step the acoustic field once in range  
 $0.13(N \log_2 N)/(10 \times 1024)$  CPU seconds where N is the  
number of depth points at which the acoustic field is  
evaluated.

Hence the total running time is

$$T = NT[28 + 1.3 \times 10^{-5} (N \log_2 N) NR] \text{ CPU seconds}$$

where

NT = Number of time steps

N = Number of depth points

NR = Number of range steps at each time.

Note: As of September 1974 the code has been changed to make use of a fast sine transform, and the eigenfunctions  $W(j,k,z)$  are being saved on disk. This has resulted in a factor-of-two increase in speed.

VIII CODE ORGANIZATION AND LISTING

Figure 8 illustrates the program flow and the FORTRAN listing of the code in its present form is given in the following pages.

```

PROGRAM USER(OUTPUT,TAPE6=OUTPUT,TAPE10)
COMMON C(30)
DIMENSION IC(30)
EQUIVALENCE(C,IC)
DIMENSION DPR(8),DBT(8)
COMMON/NFACTS/N,LN,NR,NTLOSS,NIT
COMMON/AFACTS/FREQ,SNORM,ZMAX,GW,FGW,DR,FKR,DZ,WL,PI,GO
COMMON/VAR/R,IR,T,IT
COMMON/ACOUST/UR(2048),UI(2048)
COMMON/STOP/ISTOP
COMMON/PHASES/SK(1024),CK(1024),SM(1024),CM(1024)
COMMON/BFUR/URB(1024),UIB(1024),ANGB(1024)
COMMON/MUNK/CA,ZA,ZW,GEE
COMMON/IWAVES/END,FINER,BZ,EZMAX,NZ,AKMAX,NK,NMODE,DELC,
* TIW,JSTAR
COMMON/SAV/SAVR(100,4),SAVI(100,4)
COMMON/STEP/NSTEP,ISTEP,NSAV,DT
DIMENSION LR(12),LZ(4)
DATA LR/20,40,60,80,100,120,160,200,250,320,400,500/
DATA LZ/25,102,166,256/
DATA END,FINER,NZ,AKMAX,NK,NMODE,DELC, TIW,JSTAR/
* 4.,0.04,257,1.0,128,24,0.0,2.5,6/
DATA T,IT/0.,1/
DATA CA,ZA,ZW,GEE/1500.,1300.,1300.,0.017/
DATA ISTOP/0/
DATA FREQ,GO,DPR,SNORM/100.,1300.,1000.,7*0.,1500./
DATA N,DRKM,NR,NTLOSS,ZMAX,FGW /512.,25,200,1,4000.,1./
DATA NBF /1/
DATA R,RKM /2*0./
DATA PI /3.1415926356/
R=0.
ZBF=1300.
IR=1
GU TO 60
70 CONTINUE
CALL TAPEIW(1)
DO 50 IT=1,ISTEP
MR=1
NSAV=0
R=0.
NP=0
T=DT*(IT-1)
CALL INIT
CALL PHASE1
CALL PHASE2
DO 10 IR=1,NSTEP
JR=MOD(IR,40)
IF (DELC.EQ.0.) GO TO 767
CALL PHASE2
767 CONTINUE
CALL UWS
R=R+DR
IF (MOD(IR,20).EQ.0) CALL PRINTP(UR,UI,N,R)
NSAV=NSAV+1
DO 14 IDE=1,4
IDP=LZ(IDE)
SAVR(NSAV,IDE)=UR(IDP)

```

```

14 SAVI(NSAV,IDE)=UI(IDP)
IF (IR.NE.LR(MR)) GO TO 12
MR=MR+1
CALL TAPEIW(2)
NSAV=0
12 CONTINUE
10 CONTINUE
50 CONTINUE
  WRITE(6,200)
  ISTOP=1
  CALL TAPEIW(3)
  STOP
60 CONTINUE
NSTEP=500
FREQ=100. $ N=512
DRKM=0.5
DT = 3840.
NSAV=0
DELC=.0004
ISTEP=32
BL=ZW $ EZMAX=ZMAX
TPI=2.*PI
ENO=ENO*TPI/3600.
FINER=FINER*TPI/3600.
AKMAX=AKMAX*TPI/1000.
WBF=250.
LN=ALOG(FLOAT(N))/ALOG(2.)+.5
N=2**LN
DR=DRKM*1000. $ WL=SNORM/FREQ $ FKR=2.*PI/WL
GW=FGW*WL $ DZ=ZMAX/FLOAT(N)
ZKM=ZMAX/1000.
RANGE=NSTEP*DRKM
  WRITE(6,300) FREQ,ZKM ,N,DZ,RANGE,NSTEP,DRKM
*,DELC
300 FORMAT(1H1,* ACOUSTIC FREQUENCY *,F4.0,* HZ*/
*, * OCEAN DEPTH *,F3.1,* KM NO. OF DEPTH POINTS*,I5,
*, * STEP SIZE*,F8.2,* M*/*
*, * RANGE *,F6.2,* KM NO. OF RANGE STEPS*,I5,
*, * STEP SIZE*,F5.2,* KM*/*
*, * DELC *,E12.2,/)
  WRITE(6,100)
  WRITE(6,200)
100 FORMAT(20X,*PLUT OF THE ACOUSTIC FIELD*/
*, 17X,*ALL DIMENSIONS ARE IN KILOMETERS*,*/
*, * RANGE / DEPTH ->*
*, * ?*/
*, * ?*)
200 FORMAT(1H0,9X,*0.0*9X*0.5*9X*1.0*9X*1.5*9X*2.0*
*, 9X*2.5*9X*3.0*9X*3.5*9X*4.0*)
GO TO 70
END

```

```

SUBROUTINE EIGENFN(GAMMA,K,W,WG,DZ,NL,FZN)
COMMON /EGNFN/ F(257),G(257),QN(257),QNS(257)
REAL K,KQ
DATA C6,C24/.1666666666666666,.0416666666666666/
PQ(X)=GAMMAQ*X-KQ
GAMMAQ=(DZ*GAMMA)**2
KQ=(DZ*K)**2
F(1)=F1=FZZ1=0.
FZ1=DZ
G(1)=G1=GZ1=GZZ1=0.
DO 100 I=2,NZ
F2=F1+.5*FZ1+.125*FZZ1
G2=G1+.5*GZ1+.125*GZZ1
PQ2=PQ(QN(I-1))
F2=F2-C24*(FZZ1+F2*PQ2)
G2=G2-C24*(GZZ1+G2*PQ2+F2*QN(I-1))
FZZ2=-F2*PQ2
GZZ2=-G2*PQ2-F2*QN(I-1)
F3=F1+FZ1+C6*(FZZ1+2.*FZZ2)
G3=G1+GZ1+C6*(GZZ1+2.*GZZ2)
PQ3=PQ(QN(I))
FZZ3=-F3*PQ3
GZZ3=-G3*PQ3-F3*QN(I)
F(I)=F1=F3
G(I)=G1=G3
FZ1=FZ1+C6*(FZZ1+4.*FZZ2+FZZ3)
GZ1=GZ1+C6*(GZZ1+4.*GZZ2+GZZ3)
FZZ1=FZZ3
100 GZZ1=GZZ3
W=-F1
WG=-G1*DZ**2
FZN=FZ1
RETURN
END

```

```

SUBROUTINE EIGENVL(GAMMA,K,NORM,UNORM,MODE,MERR,IERR,
•NZ,DZ,HN,LRR)
COMMON /EGNFN/ F(257),G(257),QN(257),QNS(257)
COMMON/IWAVES/ENO,FINER,A(9)
REAL K, NORM
MERR=0
IERR=0
DGMAX=.6/HN
SGN=1.
IFI(MOD(MODE,2).EQ.0) SGN=-1.
DO 10 I=1,10
CALL EIGENFN(GAMMA,K,W,WG,DZ,NZ,FZN)
IFI( SGN*WG.LE.0.) GO TO 11
DGAMMA=W/(2.*GAMMA*WG)
IFI(ABS(DGAMMA).GT.DGMAX) DGAMMA=SIGN(DGMAX,DGAMMA)
GAMMA=GAMMA-DGAMMA
IFI(ABS(DGAMMA/GAMMA).LE.ERR) GO TO 12
10 CONTINUE
11 IERR=1
12 M=1
EPS=DZ**2*W/WG
DO 20 I=1,NZ
20 F(I)=F(I)-EPS*G(I)
N1=NZ-1
DO 25 I=2,N1
IFI((F(I-1)*F(I).LT.0.).OR.F(I).EQ.0.) M=M+1
25 CONTINUE
MERR =M-MODE
IFI(MERR.NE.0.OR.IERR.EQ.1) RETURN
UNORM=-WG*FZN/DZ
RON=1./SQRT(UNORM)
SUM=0.
SUMR=0.
DO 30 I=1,NZ
SUM=SUM+F(I)**2
F(I)=F(I)*(QN(I) + FINER**2)
SUMR=SUMR + F(I)**2
30 CONTINUE
UNORM=1./SQRT(SUMR*DZ)
DO 31 I=1,NZ
31 F(I) = F(I)*UNORM
NORM=DZ*SUM
RETURN
END

```

```

SUBROUTINE FFT842(N2POW,X,Y)
DIMENSION X(2),Y(2),L(15),CS(2049),SS(2049)
EQUIVALENCE(L15,L(1)),(L14,L(2)),(L13,L(3)),(L12,L(4)),(L11,L(5)),
L(L10,L(6)),(L9,L(7)),(L8,L(8)),(L7,L(9)),(L6,L(10)),(L5,L(11)),(L4
2,L(12)),(L3,L(13)),(L2,L(14)),(L1,L(15))
DATA LST /0/
NTHPO =2**N2POW
N8POW=N2POW/3
IF(N8POW) 17,3,17
17 LNG=NTHPO
FLNG=LNG
IF (LNG-LST) 171,173,171
171 LST=LNG
DT=6.283185307179/FLNG
CS(1)=1.
SS(1)=0.
TH=0.
ND=LST/8
DO 172 I=2,ND
TH=TH+DT
CS(I)= C0S(TH)
172 SS(I)= SIN(TH)
173 DO 1 IPASS=1,N8POW
NXTLT =2** (N2POW-3*IPASS)
LENGT =8*NXTLT
SC=FLNG/FLOAT(LENGT)
DO1J=1,NXTLT
NRG=FLOAT(J-1)*SL+1.5
C1=CS(NRG)
S1=SS(NRG)
C2=C1**2-S1**2
S2=C1*S1+C1*S1
C3=C1*C2-S1*S2
S3=C2*S1+S2*C1
C4=C2**2-S2**2
S4=C2*S2+C2*S2
C5=C2*C3-S2*S3
S5=C3*S2+S3*C2
C6=C3**2-S3**2
S6=C3*S3+C3*S3
C7=C3*C4-S3*S4
S7=C4*S3+S4*C3
DO1ISQLD =LENGT ,NTHPO ,LENGT
J0=ISQLD -LENGT +J
J1=J0+NXTLT
J2=J1+NXTLT
J3=J2+NXTLT
J4=J3+NXTLT
J5=J4+NXTLT
J6=J5+NXTLT
J7=J6+NXTLT
AK0=X(J0)+X(J4)
AR1=X(J1) + X(J5)
AR2=X(J2)+X(J6)
AR3=X(J3)+X(J7)
AR4=X(J0)-X(J4)
AR5=X(J1)-X(J5)

```

```

AR6=X(J2)-X(J6)
AR7=X(J3)-X(J7)
A10=Y(J0)+Y(J4)
A11=Y(J1)+Y(J5)
A12=Y(J2)+Y(J6)
A13=Y(J3)+Y(J7)
A14=Y(J0)-Y(J4)
A15=Y(J1)-Y(J5)
A16=Y(J2)-Y(J6)
A17=Y(J3)-Y(J7)
BR0=AR0+AR2
BR1=AR1+AR3
BR2=AR0-AR2
BR3=AR1-AR3
BR4=AR4-A16
BR5=AR5-A17
BR6=AR4+A16
BR7=AR5+A17
B10=A10+A12
B11=A11+A13
B12=A10-A12
B13=A11-A13
B14=A14+AR6
B15=A15+AR7
B16=A14-AR6
B17=A15-AR7
X(J0)=BR0+BR1
Y(J0)=B10+B11
IF(J-1) 2,2,18
18 X(J1)= C4*(BR0-BR1)-S4*(B10-B11)
Y(J1)=C4*(B10-B11)+S4*(BR0-BR1)
X(J2)=C2*(BR2-B13)-S2*(B12+BR3)
Y(J2)=C2*(B12+BR3)+S2*(BR2-B13)
X(J3)=C6*(BR2+B13)-S6*(B12-BR3)
Y(J3)=C6*(B12-BR3)+S6*(BR2+B13)
TR= 0.7071067812*(BR5-B15)
T1=0.7071067812*(BR5+B15)
X(J4)=C1*(BR4+TR)-S1*(B14+T1)
Y(J4)=C1*(B14+T1)+S1*(BR4+TR)
X(J5)=C5*(BR4-TR)-S5*(B14-T1)
Y(J5)=C5*(B14-T1)+S5*(BR4-TR)
TR=-0.7071067812*(BR7+B17)
T1=0.7071067812*(BR7-B17)
X(J6)=C3*(BR6+TR)-S3*(B16+T1)
Y(J6)=C3*(B16+T1)+S3*(BR6+TR)
X(J7)=C7*(BR6-TR)-S7*(B16-T1)
Y(J7)=C7*(B16-T1)+S7*(BR6-TR)
GU TU 1
2 X(J1)=BR0-BR1
Y(J1)=B10-B11
X(J2)=BR2-B13
Y(J2)=B12+BR3
X(J3)=BR2+B13
Y(J3)=B12-BR3
TR=0.7071067812*(BR5-B15)
T1=0.7071067812*(BR5+B15)
X(J4)=BR4+TR

```

```

Y(J4)=B14+TI
X(J5)=BR4-TR
Y(J5)=B14-TI
TR=-0.7071067812*(BR7+B17)
TI=0.7071067812*(BR7-B17)
X(J6)=BR6+TR
Y(J6)=B16+TI
X(J7)=BR6-TR
Y(J7)=B16-TI
1  CONTINUE
3  IF(N2POW-3*N8POW-1)5,6,7
6  DO61J=1,NTHPO ,2
    R1=X(J)+X(J+1)
    X(J+1)=X(J)-X(J+1)
    X(J)=R1
    FI1=Y(J)+Y(J+1)
    Y(J+1)=Y(J)-Y(J+1)
61  Y(J)=FI1
    GOT05
7  DO71J1=1,NTHPO ,4
    J2=J1+1
    J3=J2+1
    J4=J3+1
    R1=X(J1)+X(J3)
    R2=X(J1)-X(J3)
    R3=X(J2)+X(J4)
    R4=X(J2)-X(J4)
    FI1=Y(J1)+Y(J3)
    FI2=Y(J1)-Y(J3)
    FI3=Y(J2)+Y(J4)
    FI4=Y(J2)-Y(J4)
    X(J1)=R1+R3
    Y(J1)=FI1+FI3
    X(J2)=R1-R3
    Y(J2)=FI1-FI3
    X(J3)=R2-FI4
    Y(J3)=FI2+R4
    X(J4)=R2+FI4
71  Y(J4)=FI2-R4
5  DO51J=1,15
    L(J)=1
    IF(J-N2POW) 19,19,51
19  L(J) = 2** (N2POW+1-J)
51  CONTINUE
    IJ=1
    DO8J1=1,L1
    DO8J2=J1,L2,L1
    DO8J3=J2,L3,L2
    DO8J4=J3,L4,L3
    DO8J5=J4,L5,L4
    DO8J6=J5,L6,L5
    DO8J7=J6,L7,L6
    DO8J8=J7,L8,L7
    DO8J9=J8,L9,L8
    DO8J10=J9,L10,L9
    DO8J11=J10,L11,L10
    DO8J12=J11,L12,L11

```

```

D08J13=J12,L13,L12
D08J14=J13,L14,L13
D08JI=J14,L15,L14
IF(IJ-JI) 20,8,8
20  R=X(IJ)
      X(IJ)=X(JI)
      X(JI)=R
      FI=Y(IJ)
      Y(IJ)=Y(JI)
      Y(JI)=FI
      8   IJ=IJ+1
      RETURN
      END

```

```

SUBROUTINE INIT
COMMON /ACOUST/ UR(2048),UI(2048)
COMMON /NFACTS/ N,LN,NR,NTLOSS,NIT
COMMON /AFACTS/ FREQ,SNORM,ZMAX,GW,FGW,DR,FKR,DZ,WL,PI,GD
PROF(X)=SGAIN*EXP(-((X-GD)/GW)**2)
SGAIN=(.9144/GW)*SQRT(WL/PI)
DO 10 J=1,N
DEPTH=DZ*FLOAT(J)
UR(J)=PROF(DEPTH)-PROF(-DEPTH)
10 UI(J)=0.
RETURN
END

```

```

SUBROUTINE PHASE1
COMMON /PHASES/ SK(1024),CK(1024),SM(1024),CM(1024)
COMMON /NFACTS/ N,LN,NR,NTLOSS,NIT
COMMON /AFACTS/ FREQ,SNORM,ZMAX,GW,FGW,DR,FKR,DZ,WL,PI,GD
FK=PI/ZMAX
FN=FLUAT(N*2)
DO 10 K=1,N
AK=FLOAT(K)*FK/FKR
ANG=.5*DR*FKR*AK**2
SK(K)=SIN(ANG)/FN
10 CK(K)=COS(ANG)/FN
RETURN
END

```

```

SUBROUTINE PHASE2
REAL SSM(1024),SSF(1024),ALOSS(1024)
COMMON /PHASES/ SK(1024),CK(1024),SM(1024),CM(1024)
COMMON /NFACTS/ N,LN,NR,NTLOSS,NIT
COMMON /AFACTS/ FREQ,SNORM,ZMAX,GW,FGW,DR,FKR,DZ,WL,PI,GD
COMMON /MUNK/ CA,ZA,ZW,GEE
DATA ISTRT /0/
IF(ISTRT .GT. 0) GOTO 100
ISTRT=1
DLW=.04*ZMAX
DLP=.05
DO 10 J=1,N
DEPTH=DZ*FLOAT(J)
BLOSS=DLP*EXP(-((DEPTH-ZMAX)/DLW)**2)
10 ALOSS(J)=EXP(-DR*BLOSS)
DO 20 J=1,N
DEPTH=DZ*FLOAT(J)
ARG=2.*((DEPTH-ZA)/ZW)
20 SSM(J)=CA+GEE*(ZW/2.)*(ARG-1.+EXP(-ARG))
DO 30 J=1,N
EN=SNORM/SSM(J)
30 SSM(J)=.5*FKR*DR*(EN+1.)*(EN-1.)
100 CONTINUE
CALL RNDMF(SSF)
DO 120 J=1,N
ANG=SSM(J)+SSF(J)
SM(J)=ALOSS(J)*SIN(ANG)
120 CM(J)=ALOSS(J)*COS(ANG)
RETURN
END

```

```

SUBROUTINE PRINTP
COMMON/ACOUST/UR(2048),UI(2048)
COMMON/NFACTS/N,LN,NR,NTLOSS,NIT
COMMON/VAR/R,IR
INTEGER PI(32)
ISK=N/32
RAN=R/1000.
DO 10 J=1,32
I=(J-1)*ISK+1
POW=UR(I)**2+UI(I)**2
10 P(J)=-10.+ ALOG10(POW/R+1.E-100)
WRITE(6,20) RAN,P,IR
20 FORMAT(F7.2,3X,32I3,15)
RETURN $ END

```

```
FUNCTION PS(K,MODE)
REAL K
COMMON /IWAVES/ EN0,FINER,BZ,EZMAX,NZ,AKMAX,NK,NMODE,
1 SIG,TIW,JSTAR
DATA ISTRT /0/
DATA PI /3.1415926536/
H(X)=(TIW-1.)*((1.+X)**(-TIW))
IF(ISTRT.NE.0) GO TO 100
ISTRT=1
S=FINER/EN0
AK0=1./BZ
AA=FLOAT(JSTAR)*PI*S*AK0
AK1=AKMAX/FLOAT(NK)
COEF=AK1*SIG**2*(BZ/3.)*(4.*S)*AK0
100 ALAM=FLOAT(MODE)/FLOAT(JSTAR)
AKREF=AA*ALAM
PS=CUEF*K**2*ALAM*H(ALAM)/(K**2+AKREF**2)**2
RETURN
END
```

```

SUBROUTINE RNDMF(SSF)
REAL SSF(1),SST(257),YZ(257),AZ(257)
COMMON /IWAVES/ EN0,FINER,B7,EZMAX,NZ,AKMAX,NK,NMODE,
1 SIG,TIW,JSTAR
LARGE EFR(256,257),EFI(256,257)
COMMON /NFACTS/ N,LN,NR,NTLOSS,NIT
COMMON /AFACTS/ FREQ,SNORM,ZMAX,GW,FGW,DR,FKR,DZ,WL,PI
COMMON /VAR/ R,IR,T,IT
REAL ESK(256),ESI(256)
REAL SP(4)
DATA ITT /0/
IF(IT.EQ.ITT) GOTO 100
ITT=IT
DO 1 I=1,N
1 SSF(I)=0.
IF(SIG.EQ.0.) GOTO 100
NX=2*NK
TPI=2.*PI
DX=PI/AKMAX
SR2=1./SQRT(2.)
FCTR=FKR*DR
DEZ=EZMAX/FLOAT(NZ-1)
RDEZS=1./DEZ**2
CALL ZMODEJ
LNX= ALOG(FLOAT(NX))/ALOG(2.)+.5
DO 2 IZ=1,NZ
DO 21 IL=1,NX
ESR(IL)=EFR(IL,IZ)
21 ESI(IL)=EFI(IL,IZ)
CALL FFT842(LNX,ESR,ESI)
DO 22 IL=1,NX
EFR(IL,IZ)=ESR(IL)
22 EFI(IL,IZ)=ESI(IL)
2 CONTINUE
DSUM=0.
L=0
DO 5 IZ=1,NZ
SUM=0.
DO 4 IX=1,NX
EFR(IX,IZ)=SR2*(EFR(IX,IZ)+EFI(IX,IZ))
4 SUM=SUM+EFR(IX,IZ)**2
SUM=SUM/FLOAT(NX)
L=L+1
SP(L)=SUM
IF(L.LT.4) GOTO 5
L=0
5 DSUM=DSUM+SUM
DSUM=DEZ*DSUM
WRITE(6,91) DSUM
90 FORMAT(1H ,15,4X,4E14.5)
91 FORMAT(1H0,* Z INTEGRAL OF DC/C SQUARED = *,E14.5,/)
IRSKP=INT(DX/DR+.1)
IZSKP=FLOAT(N)/FLOAT(NZ-1)+.5
RRSKP=1./FLOAT(IRSKP)
KZSKP=1./FLOAT(IZSKP)
AZ(1)=AZ(NZ)=YZ(1)=0.
NZI=NZ-1

```

```

100  CONTINUE
    IF(SIG.EQ.0) RETURN
    IX=MOD((IR-1)/IRSKP,NX)+1
    IXP1=IX+1 $ IF(IX.EQ.NX)IXP1=1
    IF(IRSKP.GT.1) GOTO 108
    DO 104 IZ=1,NZ
104  SST(IZ)=EFR(IX,IZ)
    GO TO 115
108  JR=MOD(IR-1,IRSKP)
    U=FLUAT(JR)*RRSKP
    V=1.-U
    DO 110 IZ=1,NZ
110  SST(IZ)=U*EFR(IXP1,IZ)+V*EFR(IX,IZ)
115  CONTINUE
    DO 120 IZ=2,NZ1
    YZ(IZ)=1./(4.-YZ(IZ-1))
    TEMP=(SST(IZ+1)-2.*SST(IZ)+SST(IZ-1))*RDEZS
120  AZ(IZ)=(TEMP-AZ(IZ-1))*YZ(IZ)
    DO 130 IB=2,NZ1
    IZ=NZ+1-IB
130  AZ(IZ)=AZ(IZ)-YZ(IZ)*AZ(IZ+1)
    DO 140 I=1,NZ1
    DO 140 J=1,IZSKP
    IZ=IZSKP*(I-1)+J
    U=FLUAT(J)*RZSKP
    V=1.-U
    SSF(IZ)=U*SST(I+1)+V*SST(I)-
    1.DZ**2*U*V*(AZ(I)*(1.+V)+AZ(I+1)*(1.+U))
140  CONTINUE
    DO 150 I=1,N
150  SSF(I)=-FCTR*SSF(I)
    RETURN
    END

```

```

SUBROUTINE TAPEIW(IFL)
COMMON/AFACTS/AF(11)
COMMON/NFACTS/BNF(5)
COMMON/MUNK/UM(4)
COMMON/IWAVES/BIW(11)
COMMON/STEP/STE(4)
COMMON/SAV/SAVR(100,4),SAVI(100,4)
COMMON/ACOUST/UR(2048),UI(2048)
COMMON/VAR/R,IR,T,IT
EQUIVALENCE (NSAV,STE(3))
DIMENSION B(2850)
GU TO (100,200,300) IFL
100 CONTINUE
L=0
DO 1 I=1,11
L=L+1
1 B(L)=AF(I)
DO 2 I=1,5
L=L+1
2 B(L)=BNF(I)
DO 3 I=1,4
L=L+1
3 B(L)=UM(I)
DO 4 I=1,11
L=L+1
4 B(L)=BIW(I)
DO 5 I=1,4
L=L+1
5 B(L)=STE(I)
WRITE(10) L,(B(I),I=1,L)
RETURN
200 CONTINUE
B(1)=R
B(2)=T
L=2
DO 31 I=1,1024
L=L+1
31 B(L)=UR(I)
DO 32 I=1,1024
L=L+1
32 B(L)=UI(I)
DO 33 I=1,4
DO 33 J=1,NSAV
L=L+1
B(L)=SAVR(J,I)
L=L+1
33 B(L)=SAVI(J,I)
WRITE(10) L,(B(I),I=1,L)
RETURN
300 CONTINUE
ENDFILE 10
ENDFILE 10
RETURN
END

```

```

SUBROUTINE UWS
COMMON /ACOUST/ UR(2048),UI(2048)
COMMON /PHASES/ SK(1024),CK(1024),SM(1024),CM(1024)
COMMON /NFACTS/ N,LN,NR,NTLOSS,NIT
COMMON /AFACTS/ FREQ,SNORM,ZMAX,GW,FGW,DR,FKR,DZ,WL,PI,G
NM1=N-1
N2=N*2
DO 10 J=1,NM1
UR(J+N)=-UR(N-J)
10 UI(J+N)=-UI(N-J)
UR(N2)=0.
UI(N2)=0.
CALL FFT842(LN+1,UR,UI)
DO 20 J=1,NM1
JP1=J+1
TEMP=CK(J)*UR(JP1)-SK(J)*UI(JP1)
UI(JP1)=-CK(J)*UI(JP1)-SK(J)*UR(JP1)
UR(JP1)=TEMP
JN2=N2+1-J
TEMP=CK(J)*UR(JN2)-SK(J)*UI(JN2)
UI(JN2)=-CK(J)*UI(JN2)-SK(J)*UR(JN2)
20 UR(JN2)=TEMP
UR(1)=UI(1)=0.
UR(N+1)=UI(N+1)=0.
CALL FFT842(LN+1,UR,UI)
DO 30 J=1,N
TEMP=CM(J)*UR(J)-SM(J)*UI(J)
UI(J)=-CM(J)*UI(J)-SM(J)*UR(J)
30 UR(J)=TEMP
RETURN
END

```

```

SUBROUTINE ZMODEJ
COMMON /IWAVES/ EN0,FINER,BZ,EZMAX,NZ,AKMAX,NK,NMODE,
1 SIG,TIW,JSTAR
LARGE EFK(256,257),EFI(256,257)
COMMON /EGNFM/ F(227),G(257),QN(257),QNS(257)
COMMON /VAR/ R,IR,T,IT
REAL TK(257),AR(256,24),AI(256,24)
REAL GSV(256,24)
REAL K,KMAX,NORM,KCY
DATA PI,ERR /3.1415926536,1.E-10/
DATA ISTRT /0/
IF(ISTRT.NE.0) GOTO 20
ISTRT=1
TPI=2.*PI
KMAX=AKMAX $ ZMAX=EZMAX
DZ=ZMAX/(NZ-1) $ DK=AKMAX/FLOAT(NK)
NK2=NK*2
DUM=0
DO 10 I=1,NZ
Z=DZ*(I-1)
TEMP=EN0*BZ*(1.-EXP(-ZMAX/BZ))-FINER**2
TEMP=AMAX1(0.,TEMP)
QN(NZ+1-I)=TEMP
10 QNS(NZ+1-I)=SQRT(TEMP)
HN=EN0*BZ*(1.-EXP(-ZMAX/BZ))
DO 12 IK=1,NK
12 TK(IK)=DX*(IK-1)
20 CONTINUE
IF(IT.NE.1) GO TO 26
DO 25 MODE=1,NMODE
DO 24 IK=1,NK2
K=DK*AMIN0(IK-1,NK2+1-IK)
POW=-2.*PS(K,MODE)*ALOG(RANF(DUM)+1.E-100)
AMP=SQRT(POW)
ANG=TPI*RANF(DUM)
AR(IK,MODE)=AMP*COS(ANG)
24 AI(IK,MODE)=AMP*SIN(ANG)
AR(NK+1,MODE)=0.
25 AI(NK+1,MODE)=0.
26 CONTINUE
DO 27 IZ=1,NZ
DO 27 IK=1,NK2
EFK(IK,IZ)=0.
27 EFI(IK,IZ)=0.
DO 30 MODE=1,NMODE
GAMMA=(FLOAT(MODE)-.25)*PI/HN
DG=DDG=0.
DO 30 IK=1,NK
K=TK(IK)
GAMMA=GAMMA+DK*(DG+.5*DDG)
IF(IT.NE.1) GAMMA=GSV(IK,MODE)
DG1=DG
CALL EGENVL(GAMMA,K,NORM,ONORM,MODE,MERR,IERR,
.NZ,DZ,HN,ERR)
IF(MERR.EQ.0.AND.IERR.EQ.0) GO TO 33
KCY=500.*K/PI
PRINT 302,MODE,KCY,MERR,IERR

```

```

302 FORMAT(//40X,29HEIGENVL FAILED TO CONVERGE AT,/
* 45X,5HMODE ,12,/45X,11HWAVENUMBER ,F 8.2/
* 45X,7HMERR = ,12/45X,7HIERR = ,12)
STOP
33  RAT=NORM/UNORM
DG=K*RAT/GAMMA
DDG=DG-DG1
IF(IK.EQ.1) DDG=DK*RAT/GAMMA
IF(IT.EQ.1) GSV(IK,MODE)=GAMMA
FIW=SQRT(FINER**2+(K/GAMMA)**2)
CW=COS(FIW*T)
SW=SIN(FIW*T)
IL=NK2+2-IK
IF(IK.EQ.1) IL=NK+1
AR1=AR(IK,MODE)
AI1=AI(IK,MODE)
AR2=AR(IL,MODE)
AI2=AI(IL,MODE)
DO 35 IZ=1,NZ
JZ=NZ+1-IZ
EFR(IK,IZ)=EFR(IK,IZ)+F(JZ)*(AR1*CW-AI1*SW)
EFI(IK,IZ)=EFI(IK,IZ)+F(JZ)*(AR1*SW+AI1*CW)
EFR(IL,IZ)=EFR(IL,IZ)+F(JZ)*(AR2*CW-AI2*SW)
35 EFI(IL,IZ)=EFI(IL,IZ)+F(JZ)*(AR2*SW+AI2*CW)
30  CONTINUE
RETURN
END

```

## LOAD MAP.

FL REQUIRED TO LOAD 147500  
 FL REQUIRED TO RUN 137000  
 INITIAL TRANSFER TO USER - 27611

## BLOCK ASSIGNMENTS.

BLOCK	ADDRESS	LENGTH	FILE
/NFACTS/	100	5	
/AFACTS/	105	13	
/VAR/	120	4	
/ACOUST/	124	10000	
/STOP/	10124	1	
/PHASES/	10125	10000	
/BFOR/	20125	6000	
/MUNK/	26125	4	
/IWAVES/	26131	13	
/SAV/	26144	1440	
/STEP/	27604	4	
USER	27610	1541	LGO
PKINTP	31351	137	LGO
TAPEIW	31510	5660	LGO
DAYFOOL	37370	170	LGO
RNDMF	37560	3135	LGO
/EGNFn/	42715	2004	
ZMODEJ	44721	45154	LGO
EIGENVL	112075	230	LGO
EIGENFN	112320	236	LGO
PS	112563	131	LGO
UWS	112714	134	LGO
INIT	113050	75	LGO
PHASE1	113145	54	LGO
PHASE2	113221	6161	LGO
FFT842	121402	11242	LGO
ACGOER	132644	10	SYSLIB
ALNLUG	132654	110	SYSLIB
ENDFIL	132764	11	SYSLIB
EXP	132775	53	SYSLIB
IBALEX	133050	31	SYSLIB
OUTPTB	133101	31	SYSLIB
OUTPTC	133132	50	SYSLIB
RANF	133202	24	SYSLIB
RBAREX	133226	57	SYSLIB
KUNSYS	133305	303	SYSLIB
SINCUS	133610	72	SYSLIB
SQRT	133702	42	SYSLIB
STATUS	133744	26	SYSLIB
TIME\$	133772	37	SYSLIB
CPUCIO	134031	506	SYSLIB
CPUSYS	134537	53	SYSLIB
KODER	134612	1235	SYSLIB
RUNIOP	136047	323	SYSLIB
SYSTM	136372	322	SYSLIB
//	136714	36	SYSLIB

PRECEDING PAGE BLANK-NOT FILMED

Appendix

CUBIC SPLINE INTERPOLATION

## Appendix

## CUBIC SPLINE INTERPOLATION

The subroutine RNDMF uses cubic splines to interpolate the velocity profiles from the coarse mesh on which the random internal wave field is computed, to the finer mesh on which the acoustic field is stored. The theory behind this is as follows.

We want an interpolation formula for the function  $v(z)$ , given the mesh points  $z_i$  ( $i = 1, 2, \dots, n+1$ ) and function values  $v_i$  ( $i=1,2,\dots,n+1$ ). Let

$$\Delta z_i = z_{i+1} - z_i , \quad i = 1, 2, \dots, n \quad (A-1a)$$

$$\Delta v_i = (v_{i+1} - v_i) / \Delta z_i , \quad i = 1, 2, \dots, n \quad (A-1b)$$

In the interval  $z_i \leq z \leq z_{i+1}$ , define the weight functions

$$w = (z - z_i) / \Delta z_i \quad (A-2a)$$

$$\bar{w} = 1 - w \quad (A-2b)$$

In each such interval, write  $v(z)$  as a cubic polynomial continuous at the mesh points as follows:

$$\begin{aligned} v(z) &= \bar{w}v_i + wv_{i+1} + (\Delta z_i)^2 [a_i(\bar{w}^3 - \bar{w}) + a_{i+1}(w^3 - w)] \\ &= \bar{w}v_i + wv_{i+1} - (\Delta z_i)^2 \bar{w}w [a_i(\bar{w}+1) + a_{i+1}(w+1)] \quad . \end{aligned} \quad (A-3)$$

The first two terms give a linear interpolation and the last terms give a second-order correction (cubic in  $z$ ) using the undetermined coefficients  $a_i$  which are essentially the second derivatives at the mesh points. From Eq. (A-3), we find

$$v'(z) = \Delta v_i + \Delta z_i \left[ -a_i (3\bar{w}^2 - 1) + a_{i+1} (3w^2 - 1) \right] , \quad (A-4)$$

$$v''(z) = 6 \left[ a_i \bar{w} + a_{i+1} w \right] . \quad (A-5)$$

Equations (A-3) and (A-5) show that the selected way of writing  $v(z)$  makes both  $v$  and  $v''$  continuous functions of  $z$  [and incidentally Eq. (A-5) shows that  $v''(z_i) = 6a_i$ ]. In order to make  $v'(z)$  continuous, we match values of  $v'(z_{i+1})$  using Eq. (A-4) in the two neighboring intervals. This yields the conditions

$$\Delta v_i + \Delta z_i (a_i + 2a_{i+1}) = \Delta v_{i+1} - \Delta z_{i+1} (2a_{i+1} + a_{i+2})$$

which can be put in the form:

$$\Delta z_i a_i + 2(\Delta z_i + \Delta z_{i+1}) a_{i+1} + \Delta z_{i+1} a_{i+2} = \Delta v_{i+1} - \Delta v_i \quad (A-6)$$

for  $i = 1, 2, \dots, n-1$ .

To make this system of linear equations for the  $a_i$  determinate, we choose  $a_1 = a_{n+1} = 0$ . This amounts to the assumption that  $v(z)$  is linear in  $z$  at the two end points of the interpolation region (top and bottom of the ocean).

Equation (A-6) is a tri-diagonal system and is most efficiently solved numerically using the "double sweep" method. Look for a solution of the form

$$a_i = r_{i+1} - s_{i+1} a_{i+1} , \quad i = 1, \dots, n \quad (A-7)$$

Substituting Eq. (A-7) into (A-8) gives recursion relations for  $r_i$  and  $s_i$  as follows:

$$a_i = \frac{1}{p_i} \left[ (\Delta v_i - \Delta v_{i-1}) - \Delta z_{i-1} r_i \right] - \frac{\Delta z_i}{p_i} a_{i+1} \quad (A-8)$$

where  $p_i = 2(\Delta v_{i-1} + \Delta v_i) - \Delta z_{i-1} s_i$ ,  $i = 2, \dots, n$ .

Combining Eqs. (A-7) and (A-8) we obtain

$$s_{i+1} = \frac{\Delta z_i}{p_i}, \quad i = 2, \dots, n, \quad (A-9)$$

$$r_{i+1} = \left| \Delta v_i - \Delta v_{i-1} - \Delta z_{i-1} r_i \right| / p_i, \quad i = 2, \dots, n. \quad (A-10)$$

The starting values of these right-sweeping recursion relations are

$r_2 = s_2 = 0$  (as follows from  $a_1 = 0$ ). The full procedure is therefore the following. Starting with  $r_2 = s_2 = 0$ , compute  $p_2$  from Eq. (A-8), then compute  $s_3$  and  $r_3$  from Eqs. (A-9) and (A-10), and again use Eq. (A-8) to compute  $p_3$ , then Eqs. (A-9) and (A-10) to compute  $s_4$  and  $r_4$ , and so on until one obtains  $s_{n+1}$  and  $r_{n+1}$ ; then use the left-sweeping recursion relation in Eq. (A-7) starting with  $a_{n+1} = 0$  to compute successively  $a_n, a_{n-1}, \dots, a_3, a_2$ .

The values of  $a_i$  computed in this way are then used in Eq. (A-3) to compute interpolated values of  $v(z)$  where needed.

A special case of this method is when  $\Delta z_i = \text{const}$  (say,  $\Delta z_i = \Delta z$ ) for all  $i$ . Equations (A-8), (A-9), and (A-10) can then be simplified to:

$$s_{i+1} = \frac{1}{4-s_i}, \quad (A-11)$$

$$r_{i+1} = \left| \left( \Delta v_i - \Delta v_{i-1} \right) / (\Delta z)^2 - r_i \right| s_{i+1} \quad , \quad (A-12)$$

for  $i = 2, \dots, n$ . Equation (A-7) is then used to compute  $a_i$ ,  
 $i = n, \dots, 2$ ; and Eq. (A-3) gives  $v(z)$  for any  $z$ .

REFERENCES

1. M. Leontovich and V. Fok, "Solution of the Problem of Propagation of Electromagnetic Waves Along the Earth's Surface by the Parabolic Equation Method," Zh. Eksp. Teor. Fiz., Vol. 16, p. 557 (1946).
2. F. D. Tappert and R. H. Hardin, in "A Synopsis of the AESD Workshop on Acoustic Modeling by Non Ray Techniques, 22-25 May 1973, Washington, D.C.," AESD TN-73-05, Office of Naval Research, Arlington, VA. (November 1973).
3. F. D. Tappert, "Parabolic Equation Method in Underwater Acoustics," J. Acoust. Soc. Am., Vol. 55, S34 (1974).
4. C. Garrett and W. Munk, Geophysical Fluid Dynamics, Vol. 2, pp. 225-264 (1972); C. Garrett and W. H. Munk, J. Geophysical Res. Vol. 80, 291 (1974); and W. H. Munk, private communication (1974).
5. W. Munk, J. Acoust. Soc. Am., Vol. 55, pp. 220-226 (1974).
6. S. M. Flatté and F. D. Tappert, "Calculation of the Effect of Internal Waves on Oceanic Sound Transmission," accepted for publication in the J. Acoust. Soc. Am..
7. M. Milder, "Users Manual for the Computer Program ZMODE," RDA-TR-2701-001, R&D Associates, Santa Monica, Calif. (July 1973).

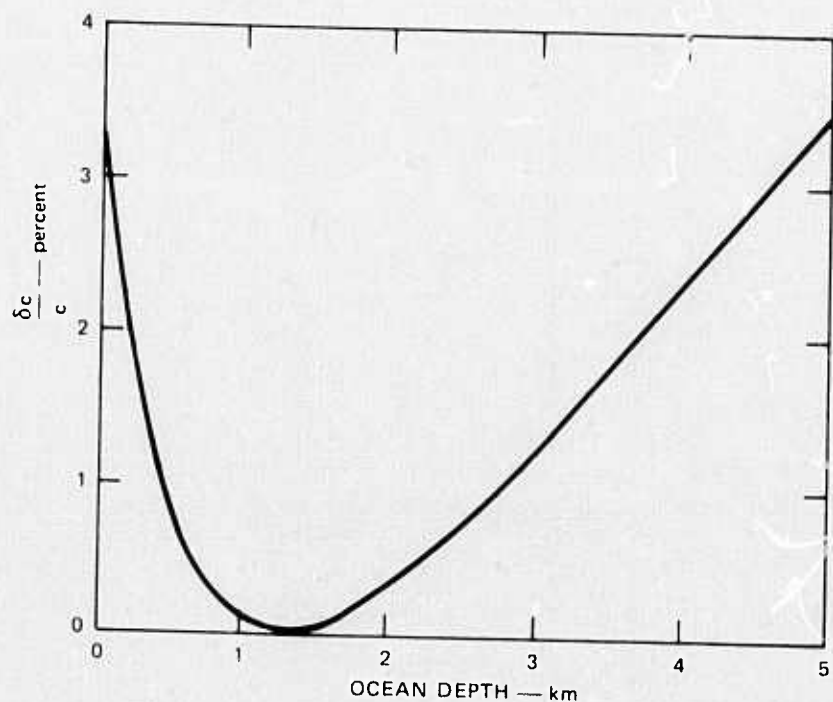


FIGURE 1 DETERMINISTIC SOUND-SPEED PROFILE AS A FUNCTION OF OCEAN DEPTH. The value of  $c$  at the minimum ( $z_A = 1300$  m) is  $c(z_A) = 1500$  m/s.

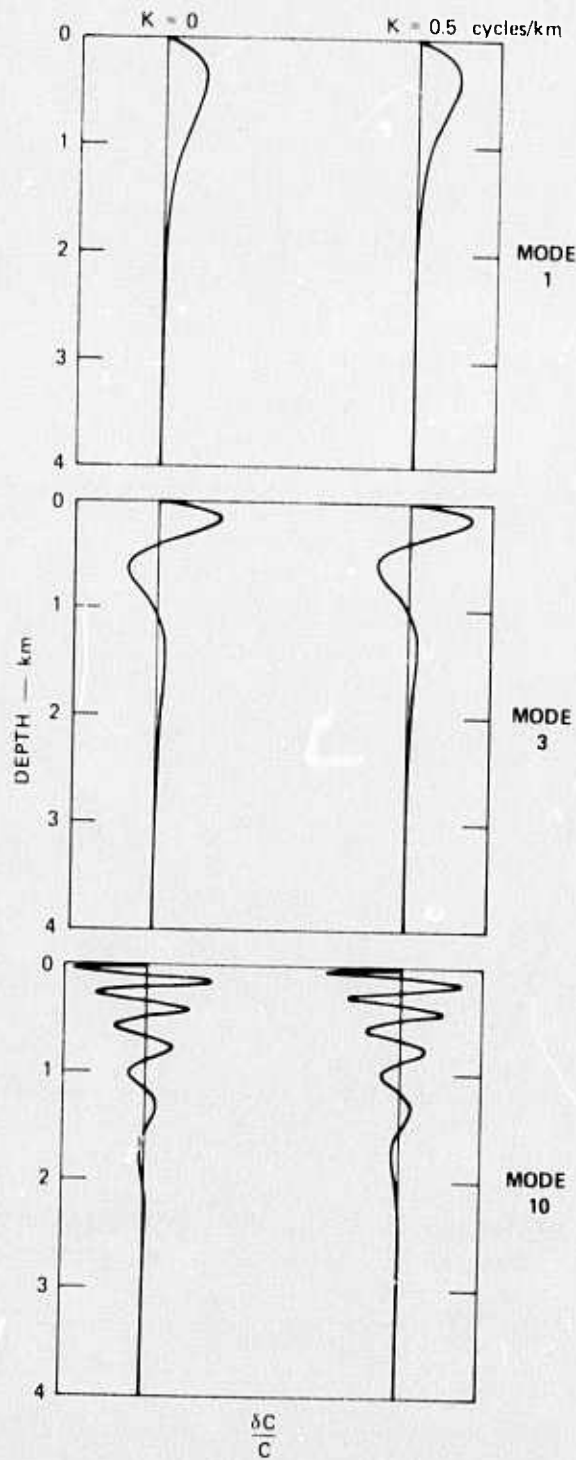


FIGURE 2 SOUND-SPEED PROFILES DUE TO INTERNAL-WAVE MODES. Realistic internal-wave spectra have significant intensities for horizontal wave number,  $k$ , less than about 0.5 cycles/km. Note that the major internal-wave contributions to sound-speed fluctuations occur at depths less than 1 km.

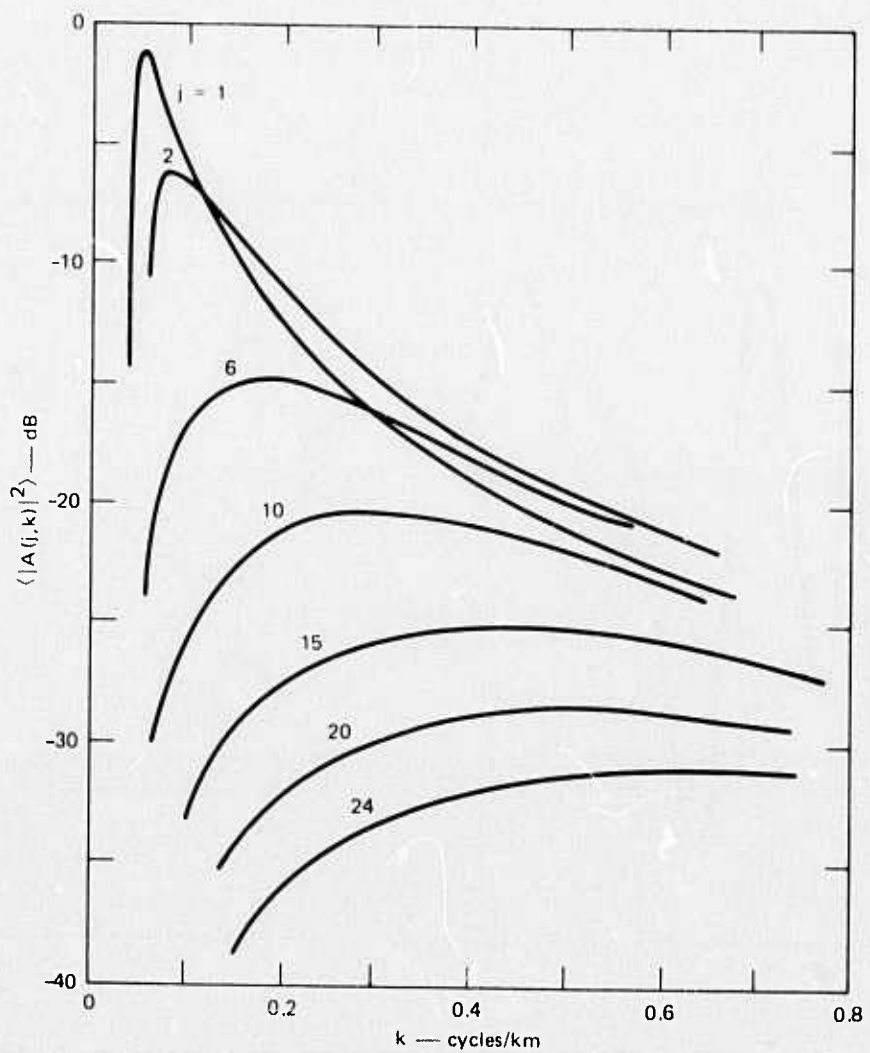


FIGURE 3 INTERNAL-WAVE SPECTRUM AS A FUNCTION OF MODE NUMBER  $j$  AND HORIZONTAL WAVE-NUMBER  $k$ . Although large mode numbers contribute very little to the overall spectrum, they are crucial to understanding acoustic effects, since their vertical structure allows them to act as a scatterer of acoustic energy more readily than the relatively structureless low modes.

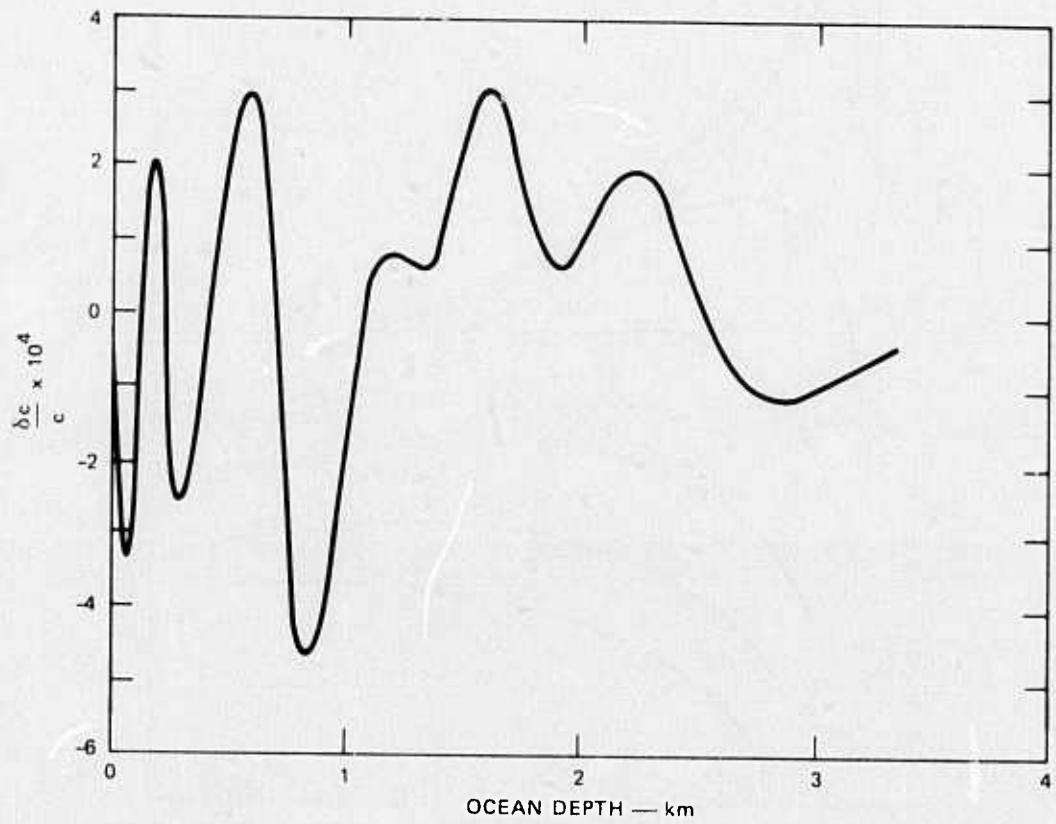


FIGURE 4 TYPICAL SOUND-SPEED FLUCTUATION PROFILE INDUCED BY INTERNAL WAVES

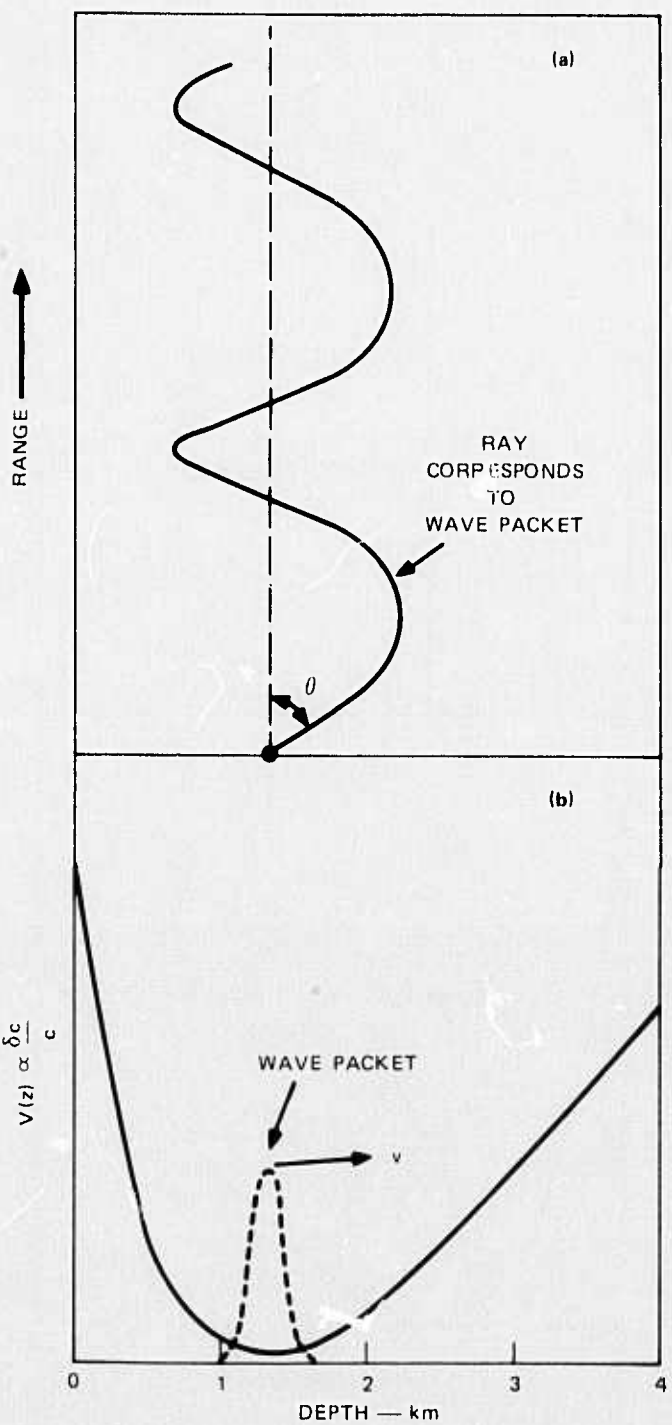


FIGURE 5 ANALOGY BETWEEN (a) AN ACOUSTIC RAY PROPAGATING IN A SOUND CHANNEL CHARACTERIZED BY  $c(z)$ , AND (b) A SCHRÖDINGER-EQUATION WAVE PACKET IN A POTENTIAL WELL  $V(z)$

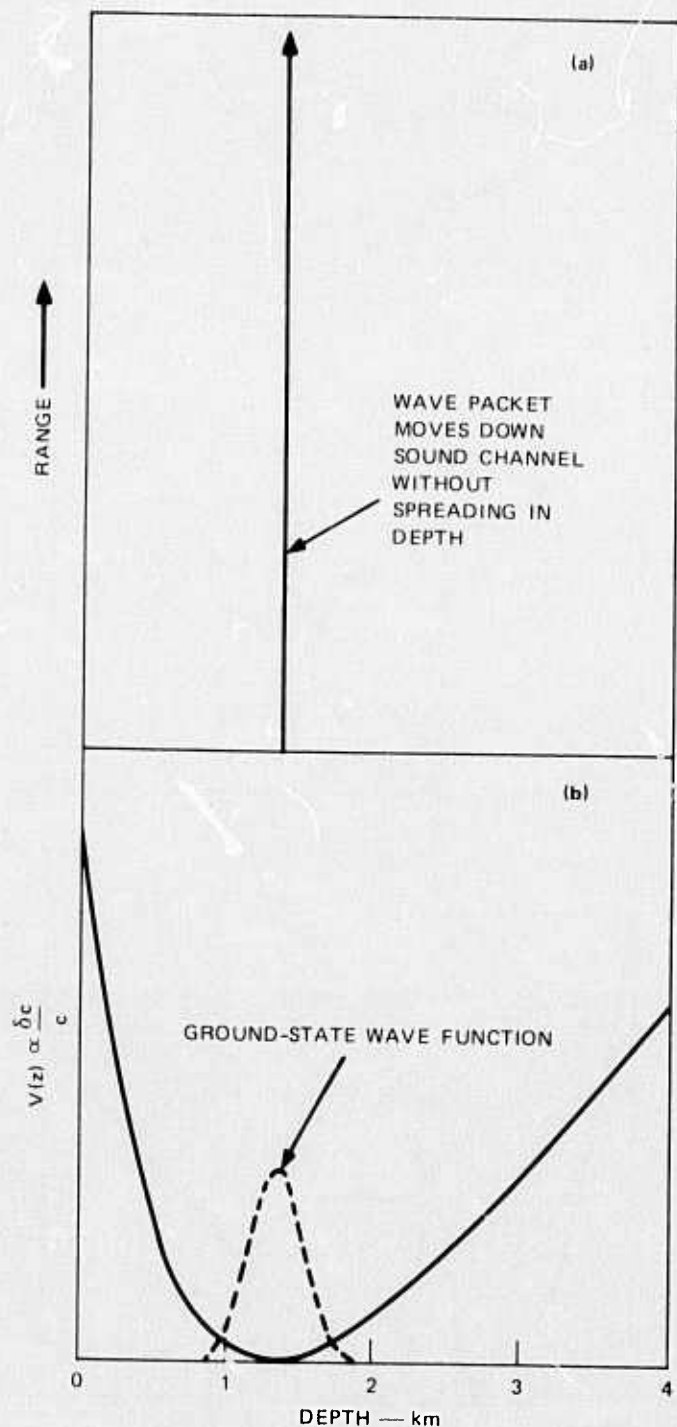


FIGURE 6 ANALOGY BETWEEN (a) AN ACOUSTIC-WAVE FUNCTION TRAVELING DOWN THE SOUND CHANNEL WITHOUT SPREADING IN DEPTH, AND (b) A SCHRÖDINGER-EQUATION GROUND-STATE WAVE FUNCTION IN A POTENTIAL WELL  $V(z)$ . Time in the Schrödinger situation corresponds to range in the acoustic case.

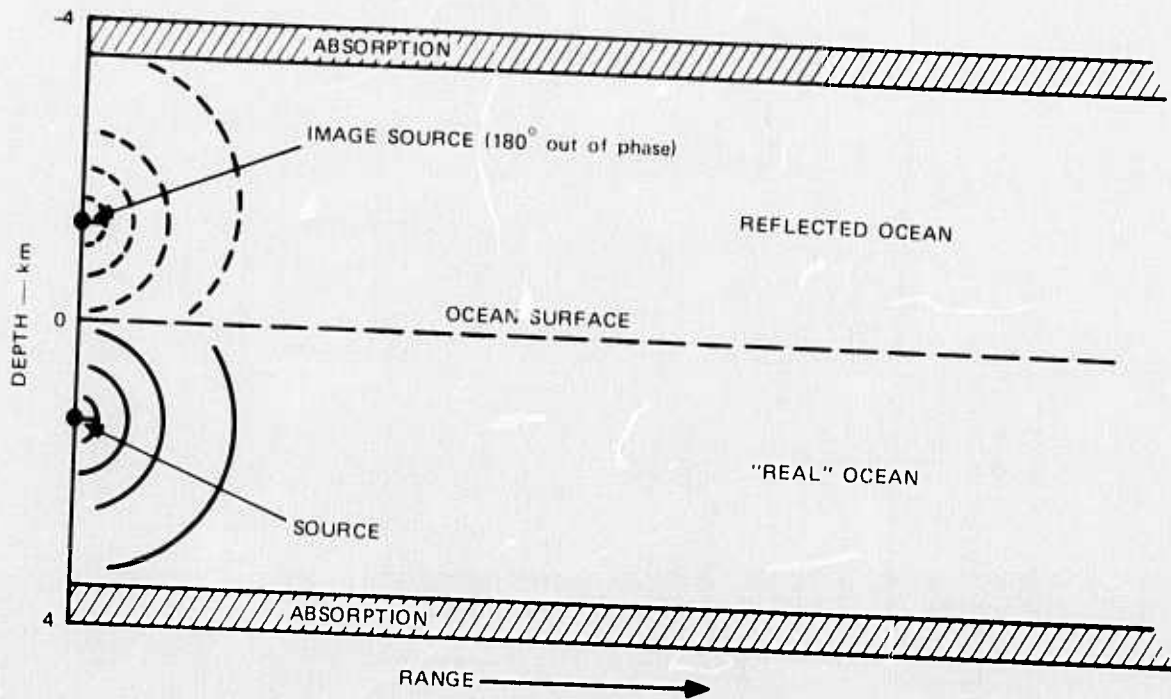


FIGURE 7 DIAGRAM OF BOUNDARY CONDITIONS AND SOURCE GEOMETRY IN OUR NUMERICAL SIMULATION. The image source in the reflected ocean automatically creates the proper ocean surface boundary condition (a perfect reflector). The absorption at the ocean bottom is a smooth function of depth, so that as little energy as possible is reflected.

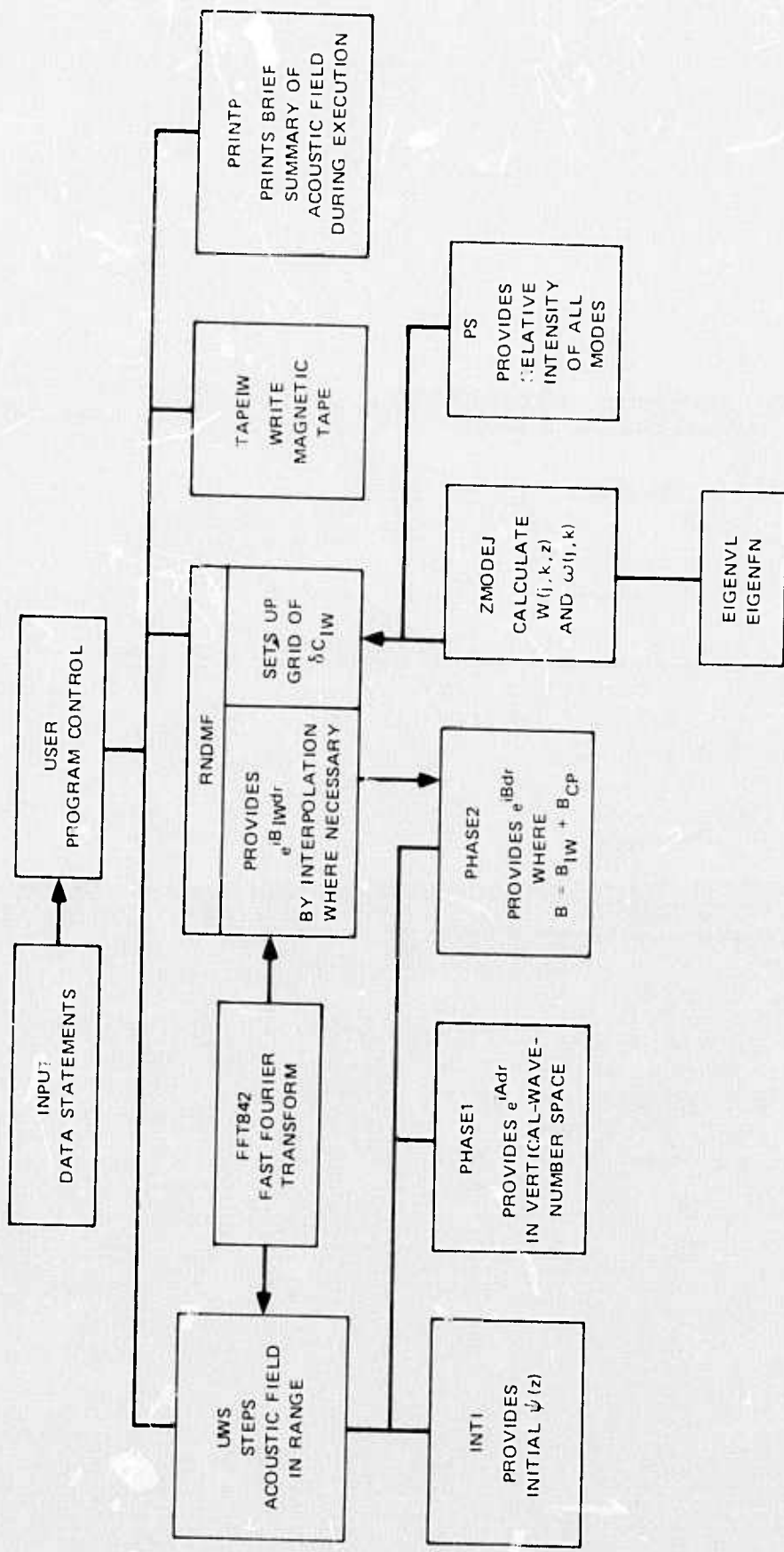


FIGURE 8 CODE ORGANIZATION

## DISTRIBUTION LIST

## DISTRIBUTION LIST

Dr. Henry D. I. Abarbanel  
 National Accelerator Laboratory  
 P.O. Box 500  
 Batavia, Illinois 60510

Aerospace Corporation  
 Attn: Dr. Thomas Taylor  
 P.O. Box 5866  
 San Bernardino, California 92408

Dr. A. L. Anderson  
 Applied Research Laboratory  
 University of Texas  
 P.O. Drawer 8029  
 Austin, Texas 78712

Dr. V. C. Anderson  
 Scripps Institution of Oceanography  
 University of California  
 La Jolla, California 92037

Applied Research Laboratory  
 Pennsylvania State University  
 Attn: W. Baker  
 H. M. Jensen  
 S. McDaniel  
 Dr. H. S. Piper  
 D. C. Stickler  
 P.O. Box 30  
 State College, Pennsylvania 16801

Capt. J. C. Bajus Code 03  
 Naval Electronic Systems Command Hqds.  
 Department of the Navy  
 Washington, D.C. 20360

Dr. R. W. Bannister  
 Defense Scientific Establishment  
 HMNZ Dockyard, Devonport  
 Auckland 45400, New Zealand

Bell Telephone Laboratories  
 Attn: R. Hardin  
 R. Holford  
 T. E. Talpey  
 Whippany, New Jersey 07901

Dr. H. F. Bezdek  
 Office of Naval Research (480)  
 Department of the Navy  
 Arlington, Virginia 22217

Prof. Theodore G. Birdsall, Director  
 Cooley Electronics Laboratory  
 Cooley Bldg., North Campus  
 University of Michigan  
 Ann Arbor, Michigan 48105

Dr. Martin H. Bloom  
 Polytechnic Institute of Brooklyn  
 Route 110, Room 205  
 Farmingdale, New York 11735

Cmdr. A. G. Brookes, Jr.  
 Office of Naval Research (Code 102-OS)  
 Department of the Navy  
 Arlington, Virginia 22217

Brown University  
 Department of Mathematics  
 Attn: C. Dafermos  
 W. Strauss  
 Providence, Rhode Island 02912

Mr. D. G. Browning  
 New London Laboratory  
 Naval Underwater Systems Center  
 New London, Connecticut 06320

Mr. B. M. Buck  
 Polar Research Laboratory, Inc.  
 123 Santa Barbara St.  
 Santa Barbara, California 93101

California Institute of Technology  
 Attn: Dr. Milton Plesset  
 Dr. Toshi Kubota  
 1201 East California Blvd.  
 Pasadena, California 91109

Dr. Curtis G. Callan, Jr.  
 Department of Physics  
 Princeton University  
 Princeton, New Jersey 08540

Dr. G. F. Carrier  
 Harvard University  
 Pierce Hall  
 Cambridge, Massachusetts 02139

Catholic University  
 Attn: F. Andrews  
 H. Uberall  
 620 Michigan Ave., NE  
 Washington, D.C. 20017

Courant Institute  
Attn: D. Ahluwalia  
C. Aquista  
J. Bazer  
R. Burridge  
J. Keller  
C. Morawetz  
G. Papanicolaou  
P. Sulem  
J. Weileman  
251 Mercer St.  
New York, New York 10012

Capt. C. G. Darrell  
Director, Undersea Warfare Technology  
Office of Naval Research (Code 412)  
Arlington, Virginia 22217

Dr. Roger F. Dashen  
Institute for Advanced Study  
Princeton, New Jersey 08540

Defence Research Establishment  
Atlantic  
Attn: Mr. J. B. Franklin  
Dr. R. S. Thomas  
P.O. Box 1012  
Dartmouth, Nova Scotia, Canada

Defence Research Establishment  
Pacific  
Department of National Defence  
Attn: Dr. R. P. Chapman  
Mr. J. M. Thorliefson  
Forces Mail Office  
Victoria, B.C., V0S 1B0, Canada

Defense Advanced Research Projects  
Agency  
Attn: Mr. Robert M. Chapman, TTO  
Mr. Craig W. Hartsell, Jr., STO  
Dr. George H. Heilmeyer, Director  
Dr. Richard F. Hoglund, TTO  
Dr. Donald J. Loft, Dep. Director  
Mr. Robert A. Moore, TTO  
Dr. Stephen Zakanycz  
1400 Wilson Boulevard  
Arlington, Virginia 22209

Prof. I. Dyer  
MIT  
Department of Ocean Engineering  
Cambridge, Massachusetts 02139

Prof. Freeman J. Dyson  
Institute for Advanced Study  
Princeton, New Jersey 08540

Dr. Harlow Farmer  
P.O. 1925 (Main Station)  
Washington, D.C. 20013

Dr. F. Fisher  
Scripps Institution of Oceanography  
University of California, San Diego  
La Jolla, California 92037

Dr. R. M. Fitzgerald  
Naval Research Laboratory  
Department of the Navy  
Washington, D.C. 20375

Dr. Stanley M. Flatté  
360 Moore St.  
Santa Cruz, California 95064

Flow Research, Inc.  
Attn: Dr. Denny R. S. Ko  
Dr. Michael Y. H. Pao  
1810 South Central Ave.  
Suite 72  
Kent, Washington 98031

General Research Corp.  
Attn: Mr. P. Donohoe  
1501 Wilson Blvd.  
Suite 700  
Arlington, Virginia 22209

George Washington University  
Computer Science and E.E.  
Attn: R. Lang  
Washington, D.C. 20006

Dr. R. R. Goodman Code 8000  
Associate Director of Research  
Naval Research Laboratory  
Department of the Navy  
Washington, D.C. 20375

Mr. W. Griswold  
U.S. Naval Ship Research and  
Development Center  
Annapolis, Maryland 21402

Mr. I. Hagan  
Royal Australian Navy Research  
Laboratory  
New Beach Road  
Edgecliff, NSW, Australia 2027

Mr. G. R. Hamilton, Director  
Ocean Science and Technology Division  
Office of Naval Research  
Department of the Navy  
Arlington, Virginia 22217

Dr. J. S. Hanna  
Office of Naval Research (AESD)  
Department of the Navy  
Arlington, Virginia 22217

Hawaii Institute of Geophysics  
University of Hawaii  
Attn: Dr. W. E. Hardy  
Mr. P. M. Volk  
2525 Correa Rd.  
Honolulu, Hawaii 96822

Dr. J. B. Hersey  
Bldg. 58  
Naval Research Laboratory  
Washington, D.C. 20390

Dr. C. W. Horton, Sr.  
Applied Research Laboratory  
University of Texas  
P.O. Drawer 8029  
Austin, Texas 78712

Dr. Norden Hueng  
Department of Geosciences  
North Carolina State University  
Raleigh, North Carolina 27607

Hydronautics, Inc.  
Attn: Dr. O. M. Phillips  
Dr. T. R. Sundaram  
Dr. J. Wu  
Pindell School Rd., Howard Co.  
Laurel, Maryland 20810

Imperial College  
Department of E.E.  
Attn: R. Clarke  
Exhibition Road  
London SW7, England

Institute for Acoustical Research  
University of Miami  
Attn: Dr. J. G. Clark  
Dr. Martin Kronengold, Director  
615 SW Second Ave.  
Miami, Florida 33130

Institute for Defense Analysis  
Attn: Dr. Joel Bengston  
Mr. J. C. Nolen  
Dr. Philip A. Selwyn  
400 Army-Navy Drive  
Arlington, Virginia 22202

Frank Jablonski (OPNAV)  
Room 4B489  
The Pentagon  
Washington, D.C. 20350

Capt. D. M. Jackson  
Naval Electronic Systems  
Command Hdqs.  
PME-124  
Washington, D.C. 20360

Johns Hopkins University  
Applied Physics Laboratory  
Attn: L. Cronvich  
H. Gilreath  
N. Nicholas  
A. Stone  
8621 Georgia Ave.  
Silver Spring, Maryland 20910

Dr. I.S.F. Jones  
Head, Ocean Science Group  
Royal Australian Navy Research  
Laboratory  
New Beach Road  
Edgecliff, NSW, Australia 2027

Lamont-Doherty Geological Observatory  
Columbia University  
Attn: Mr. J. I. Ewing  
Dr. H. Kutshale  
Palisades, New York 10964

Dr. Frank Lane  
KLD Associates, Inc.  
7 High St., Suite 204  
Huntington, New York 11743

Dr. W. S. Lewellen  
Aeronautical Research Associates  
of Princeton, Inc.  
50 Washington Rd.  
Princeton, New Jersey 08540

Dr. Harold W. Lewis  
Department of Physics  
University of California  
Santa Barbara, California 93106

Mr. P. H. Lindop  
Admiralty Research Laboratory  
 Teddington, Middlesex  
England

Dr. S. W. Marshall  
 Naval Research Laboratory  
 Department of the Navy  
 Washington, D.C. 20375

Massachusetts Institute of Technology  
 Department of Mechanical Engineering  
 Attn: Dr. Eric L. Mollo-Christenson  
 Cambridge, Massachusetts 02139

Massachusetts Institute of Technology  
 Lincoln Laboratory  
 Attn: Dr. Charles W. Rook  
 P.O. Box 73  
 Lexington, Massachusetts 02173

Prof. H. Medwin  
 Naval Postgraduate School  
 Department of Physics  
 Monterey, California 93940

Cmdr. R. Miller (OPNAV)  
 Room 5D572  
 The Pentagon  
 Washington, D.C. 20390

Dr. G. A. Morgan  
 Embassy of Australia  
 1601 Massachusetts Ave., NW  
 Washington, D.C. 20036

Dr. W. Moseley Code 8160  
 Naval Research Laboratory  
 Department of the Navy  
 Washington, D.C. 20375

Dr. Walter H. Munk  
 9530 La Jolla Shores Drive  
 La Jolla, California 92037

NATO  
 SACLANT ASW Research Center  
 Attn: Dr. Bruce Williams  
 Dr. D. Wood  
 Viale San Bartolomeo, 400  
 I-19026 La Spezia, Italy

Naval Air Development Center  
 Attn: C. Bartberger  
 E. P. Garabed Code 2052  
 Warminster, Pennsylvania 18974

Naval Air Systems Command  
 Main Navy Bldg.  
 Attn: I. H. Gatzke  
 Washington, D.C. 20360

Naval Oceanographic Office  
 Attn: Mr. W. H. Geddes  
 Dr. M. Schulkin  
 Suitland, Maryland 20373

Naval Ordnance Laboratory  
 White Oak  
 Attn: I. Blatstein  
 Ms. E. A. Christian  
 R. J. Urick  
 Silver Spring, Maryland 20910

Naval Research Laboratory  
 Attn: R. Baer F. Ingenito  
 A. Berman Frank MacDonald  
 J. Cybulsky J. McCoy  
 J. Dugan S. Piacsek  
 J. O. Elliot K. G. Williams  
 B. Hurdle  
 4555 Overlook Ave., SW  
 Washington, D.C. 20390

Naval Scientific and Technical  
 Intelligence Center  
 Attn: Capt. J. P. Prisley  
 4301 Suitland Rd.  
 Washington, D.C. 20390

Naval Ship Systems Command  
 TRIDENT Project Officer  
 Washington, D.C. 20360

Naval Undersea Center  
 Attn: H. S. Aurand, Jr., Head,  
 Ocean Acoustics Division  
 Dr. H. Bucker J. Neubert  
 Dr. A. G. Fabula M. A. Pedersen  
 E. Floyd C. Ramstedt  
 D. Gordon D. White  
 H. Morris  
 San Diego, California 92132

Naval Undersea Systems Center  
 Attn: Dr. J. D'Albora  
 Newport, Rhode Island 02840

Naval Underwater Systems Center  
New London Laboratory  
Attn: D. Abraham A. Krulisch  
D. G. Browning R. Lauer  
J. Cohen G. Leibiger  
H. Cox R. L. Martin  
R. Deavenport R. H. Mellen  
F. Dinapoli J. Papadakis  
L. Einstein W. I. Roderick  
A. Ellin thorpe R. Saenger  
R. Elswick P. Scully-Power  
H. Freese D. Shonning  
O. D. Grace L. Stallworth  
J. Hassab W. A. Von Winkle  
E. Jensen H. Weinberg  
W. Kanabis  
New London, Connecticut 06320

Dr. William A. Nierenberg  
Scripps Institution of Oceanography  
University of California  
La Jolla, California 92037

ODDR&E  
The Pentagon  
Attn: G. Cann, Rm. 3D1048  
Dr. D. R. Heebner, Rm 3E1040  
N. F. Wikner, Rm 3E1087  
Washington, D.C. 20391

Office of Naval Research  
Attn: Dr. W. J. Condell  
Mr. A. O. Sykes, Code 412  
800 N. Quincy St.  
Arlington, Virginia 22217

Office of Naval Research  
Attn: D. Cacchione  
495 Summer St.  
Boston, Massachusetts 22210

Office of Naval Research  
Acoustic Environmental Support  
Detachment  
Attn: R. Buchal  
Dr. R. C. Cavanagh  
A. Cecelski  
S. Reed, Jr.  
C. W. Spofford  
Lcdr. B. T. Steele  
Cdr. P. R. Tatro, Head  
Arlington, Virginia 22217

Office of Naval Research  
Department of the Navy  
Attn: Cdr. J. Ballou  
M. Cooper  
R. Cooper  
J. Witting  
Washington, D.C. 20360

Physical Dynamics, Inc.  
Attn: Dr. Alex Thomson  
Dr. Bruce West  
P.O. Box 1069  
Berkeley, California 94704

Capt. Daniel Piraino (NSP)  
SP202  
Department of the Navy  
Washington, D.C. 20390

Polytechnic Institute of New York  
Department of Mathematics  
Attn: H. Hockstadt  
333 Jay St.  
Brooklyn, New York 11201

James H. Probus (OASN)  
Room 4E741  
The Pentagon  
Washington, D.C. 20350

R&D Associates  
Attn: Dr. F. L. Fernandez  
Dr. D. Holliday  
Dr. M. Milder  
P.O. Box 3580  
Santa Monica, California 90403

Dr. Gordon Raisbeck  
Arthur D. Little, Inc.  
Cambridge, Massachusetts 02140

Rensselaer Polytechnic Institute  
Department of Mathematics  
Attn: M. Jacobson  
Troy, New York 12181

Riverside Research Institute  
Attn: Dr. Marvin King  
80 West End Ave.  
New York, New York 10023

Mr. D. A. Rogers (NSP)  
SP2018  
Department of the Navy  
Washington, D.C. 20390

Mr. Benjamin Rosenberg (OPNAV)  
Room 4B513  
The Pentagon  
Washington, D.C. 20350

Rosentiel School of Marine and  
Atmospheric Science  
University of Miami  
Attn: Dr. S. C. Daubin  
Dr. H. DeFarrari  
Miami, Florida 33149

Dr. Donald Ross  
Tetra Tech, Inc.  
3559 Kenyon Street  
San Diego, California 92110

Science Application, Inc.  
Attn: H. Wilson  
P.O. Box 351  
La Jolla, California 92037

Mr. Carey Smith  
Naval Sea Systems Command Hdqs.  
Code 06H11  
Department of the Navy  
Washington, D.C. 20360

Stanford Research Institute  
Attn: N. Cianos, 44  
H. Guthart, 404B  
R. C. Honey, 406A  
K. Krishnan, K1068  
333 Ravenswood Ave.  
Menlo Park, California 94025

TRW Systems Group  
Attn: E. Baum  
J. Chang  
One Space Park  
Redondo Beach, California 90278

Dr. F. Tappert  
Courant Institute  
251 Mercer St.  
New York, New York 10012

Dr. C. M. Tchen  
1380 Riverside Drive  
New York, New York 10033

University of California  
Lawrence Radiation Laboratory  
Attn: Dr. Harold P. Smith  
Dr. M. Wirth  
P.O. Box 808  
Livermore, California 94550

University of California, San Diego  
Attn: Dr. C. Cox  
Dr. R. Davis  
Dr. C. Gibson  
Dr. J. Miles  
P.O. Box 119  
La Jolla, California 92038

University of California  
Scripps Institution of Oceanography  
Marine Physical Laboratory  
Attn: Dr. T. Foster  
Dr. G. B. Morris  
Dr. F. Spiess  
San Diego, California 92152

University of Rhode Island  
Attn: G. Ladas E. Roxin  
L. LeBlanc R. Suryanarayan  
F. Middleton G. Verma  
A. Poularicas  
Kingston, Rhode Island 02881

Dr. Roberto Vaglio-Laurin  
Advanced Technology Laboratories, Inc.  
400 Jericho Turnpike  
Jericho, New York 11753

Virginia Polytechnic Institute  
State University  
Attn: I. Rozieris  
W. Kohler  
Blacksburg, Virginia 24061

Cdr. Don Walsh (OASN/R&D)  
Room 4E741  
The Pentagon  
Washington, D.C. 20350

Dr. Kenneth M. Watson  
Lawrence Berkeley Laboratory  
University of California  
Berkeley, California 94720

Wayne State University  
Department of Mathematics  
Attn: P. Chow  
Detroit, Michigan 46202

Dr. M. S. Weinstein  
Underwater Systems, Inc.  
8121 Georgia Ave., Suite 700  
Silver Spring, Maryland 20910

Western Electric Co.  
Bell Telephone Laboratories  
Attn: Dr. E. Y. Harper  
Dr. F. Labianca  
Whippany, New Jersey 07981

M. Wilson  
Naval Ship Research and Development  
Center  
Washington, D.C. 20007

Woods Hole Oceanographic Institution  
Attn: Dr. E. E. Hays  
Dr. R. Porter  
Dr. R. Spindel  
Mr. W. A. Watkins  
Woods Hole, Massachusetts 02543

Dr. J. L. Worzel  
Marine Science Institute  
Geophysics Laboratory  
700 Thestrand  
Galveston, Texas 77550

Dr. D. V. Wyllie  
Weapons Research Establishment  
Box 2151, G.P.O.  
Adelaide, South Australia 5001

Dr. H. Yura  
Aerospace Corporation  
P.O. Box 92956  
Los Angeles, California 90009

Dr. Fredrik Zachariasen  
#452-48  
Department of Physics  
California Institute of Technology  
Pasadena, California 91109